



Deposited via The University of Leeds.

White Rose Research Online URL for this paper:

<https://eprints.whiterose.ac.uk/id/eprint/122914/>

Version: Accepted Version

Article:

Liu, W, Li, X, Zhang, F et al. (2017) Interactive travel choices and traffic forecast in a doubly dynamical system with user inertia and information provision. *Transportation Research, Part C: Emerging Technologies*, 85. pp. 711-731. ISSN: 0968-090X

<https://doi.org/10.1016/j.trc.2017.10.021>

(c) 2017, Elsevier Ltd. This manuscript version is made available under the CC BY-NC-ND 4.0 license <https://creativecommons.org/licenses/by-nc-nd/4.0/>

Reuse

Items deposited in White Rose Research Online are protected by copyright, with all rights reserved unless indicated otherwise. They may be downloaded and/or printed for private study, or other acts as permitted by national copyright laws. The publisher or other rights holders may allow further reproduction and re-use of the full text version. This is indicated by the licence information on the White Rose Research Online record for the item.

Takedown

If you consider content in White Rose Research Online to be in breach of UK law, please notify us by emailing eprints@whiterose.ac.uk including the URL of the record and the reason for the withdrawal request.

Interactive travel choices and traffic forecast in a doubly dynamical system with user inertia and information provision

Wei Liu^a, Xinwei Li^b, Fangni Zhang^{c,*}, Hai Yang^b

^a *School of Engineering, University of Glasgow, Glasgow G12 8LT, United Kingdom*

^b *Department of Civil and Environmental Engineering, The Hong Kong University of Science and Technology, Hong Kong, PR China*

^c *Institute for Transport Studies, University of Leeds, Leeds LS2 9JT, United Kingdom*

Abstract

This study models the joint evolution (over calendar time) of travelers' departure time and mode choices, and the resulting traffic dynamics in a bi-modal transportation system. Specifically, we consider that, when adjusting their departure time and mode choices, travelers can learn from their past travel experiences as well as the traffic forecasts offered by the smart transport information provider/agency. At the same time, the transport agency can learn from historical data in updating traffic forecast from day to day. In other words, this study explicitly models and analyzes the dynamic interactions between transport users and traffic information provider. Besides, the impact of user inertia is taken into account in modeling the traffic dynamics. When exploring the convergence of the proposed model to the dynamic bi-modal commuting equilibrium, we find that appropriate traffic forecast can help the system converge to the user equilibrium. It is also found that user inertia might slow down the convergence speed of the day-to-day evolution model. Extensive sensitivity analysis is conducted to account for the impacts of inaccurate parameters adopted by the transport agency.

Keywords: Bottleneck model; day-to-day dynamics; traffic forecast; bi-modal; user inertia.

*Corresponding author. f.zhang@leeds.ac.uk (F. Zhang)

1 Introduction

The within-day dynamic traffic patterns have been essentially characterized by the travelers' trip-timing choices and much has been modeled in the framework of the bottleneck model firstly proposed by [Vickrey \(1969\)](#). Later, [Smith \(1984\)](#) and [Daganzo \(1985\)](#) respectively established the existence and uniqueness of the user equilibrium solution in the presence of a single bottleneck, and [Arnott et al. \(1990\)](#) analyzed the departure/arrival equilibrium with piece-wise linear schedule delay cost functions. The original bottleneck model has been extended in a broad range of directions to incorporate exogenous factors such as user heterogeneity, demand and capacity uncertainty, and carpooling ([Arnott et al., 1994](#); [Xiao et al., 2013, 2016](#)), congestion and/or parking pricing ([Laih, 1994](#)), or to cater for traffic complications such as hyper-congestion and capacity drop ([Liu and Geroliminis, 2016](#); [Liu et al., 2015](#)) (one may refer to [Small, 2015](#), for a recent review). In particular, the bottleneck model has been embedded into the bi-modal transportation system to simultaneously model travelers' mode-shifting and trip-timing choices. In this context, various regulatory issues have been considered, including road pricing ([Tabuchi, 1993](#); [Wu and Huang, 2014](#)), parking space limitation ([Yang et al., 2013](#); [Liu et al., 2014](#)), and preventing the counterproductive Downs-Thomson Paradox ([Wang et al., 2017](#)).

The day-to-day traffic dynamics, however, refer to the system variations that occur between successive reference periods, which can be either the whole day or one part of a day, e.g., the morning peak period ([Cascetta and Cantarella, 1991](#)). The literature has established evidences for traffic variations from day to day, for example, [Guo and Liu \(2011\)](#). This raises the interest to model the day-to-day traffic evolution dynamics in the transportation systems. As summarized by [Yang and Zhang \(2009\)](#), the five major dynamical systems to formulate the day-to-day traffic dynamics are the proportional swap system, the network tatonnement process, the simplex gravity flow dynamics, the projected dynamical system, and the evolutionary traffic dynamics. As mentioned in [Guo and Huang \(2016\)](#), the day-to-day models have been considered in the context of Wardrop user equilibrium, Logit-based stochastic user equilibrium, or boundedly rational user equilibrium. The day-to-day dynamical system can capture the evolution process of traffic dynamics, and thus can help observe and uncover features not available in stationary models. Many studies also proposed strategies to accommodate the day-to-day traffic dynamics and thus improve system traffic efficiency ([Sandholm, 2002](#); [Smith and Mounce, 2011](#); [Guo et al., 2015](#); [Tan et al., 2015](#); [Ye et al., 2015](#); [Xu et al., 2016](#)).

Some researchers have integrated the bottleneck model into the day-to-day framework, and developed a so-called doubly dynamical system ([Ben-Akiva et al., 1984, 1986](#); [Iryo, 2008](#);

Wu, 2009; Guo et al., 2017a). The doubly dynamical system can describe the day-to-day evolution of the within-day dynamic traffic patterns. However, little has been said about the convergence of the evolution process to the dynamic user equilibrium. Recently, the non-convergence of the proportional swap system when it is applied to a bottleneck model based doubly dynamical system was shown by both Iryo (2008) and Guo et al. (2017a). Their analysis, while providing interesting insights, fails to capture several important aspects of a real transportation system including, but not limited to, how information provision or traffic forecast can affect users' travel behavior and the system dynamics; how the potentially existing user inertia might play a role in traffic evolution; and more importantly, how the multi-modality could influence users' choices and the system dynamics. While the existing studies on the day-to-day dynamical systems (include those for the doubly dynamical systems) often focus on an isolated highway system, the mode-shifting dynamics have received very little attention except from Cantarella et al. (2015), Li and Yang (2016) and Liu and Geroliminis (2017), in which the trip-timing decision is, however, not considered.

This study aims to fill these research gaps by considering a multi-modal transport system where the travelers adjust their choices of both departure time and travel mode from day to day. Particularly, we have modeled and analyzed how information provision/traffic forecast (from transport agency) and user inertia could affect travelers' choice in a day-to-day context. Note that advanced traveler information systems have been considered by Huang et al. (2008) in a day-to-day context, where the main focus is about how pre-trip information could help reduce the drivers' travel time uncertainty. Differently, in this paper in order to characterize the impact of traffic forecast on travel behavior, a more general learning process has been proposed with respect to that in Bie and Lo (2010) and Watling (1999). In such a process, the forecast travel costs provided by a transport agency are referred to in the travelers' perception updating. Furthermore, a proportional-swap-based dynamical system is developed to describe the day-to-day flow adjustment. Besides, user inertia is captured by imposing constraints on the proportional-swap system, under which users can only change their departure time within a certain amount of time between any two consecutive days. The convergence of the dynamical system described in the above towards the bi-modal dynamic user equilibrium has been explored and compared with the observations in Iryo (2008) and Guo et al. (2017a).

As mentioned in the above, user inertia is considered in the decision process for the travelers. In the context of social and behavioral sciences, inertia is generally regarded as the endurance of stable relationships or reluctance in adjustment of status quo. "Absent other forces, inertia describes the tendency to remain with the status quo and the resistance to strategic renewal outside the frame of current strategy" (Huff et al., 1992). Recent studies

have looked into the user inertia in route choices of travelers (Zhang and Yang, 2015), where travelers’ route sets might be smaller than the set of all possible routes. This paper considers a similar concept that travelers departing at a time point may only shift to a departure time that belongs to a subset of all feasible departure times in the next day. The user inertia is related to user bounded rationality (Zhang and Yang, 2015), where bounded rationality refers to that when making decisions, individual’s rationality is limited due to many factors. However, the modeling of user inertia in this paper is different from the boundedly rational user equilibrium considered in the literature (Di et al., 2013). In those papers, travelers’ choices are bounded rational for that some indifference bands exist between the costs of their own choice and the shortest route. However, travelers’ choices are not limited to a subset that is specified in the first place (or predetermined), which is the key difference from the inertia model. In summary, user inertia and bounded rationality are inter-correlated but not equivalent. A route choice model trying to incorporate different behavior assumptions is presented in Xu et al. (2017).

Furthermore, the traffic forecast of the transport agency is based on an auxiliary day-to-day learning model and a traffic simulator with the observed data being the input and the cost estimates for travelers being the output. This learning model coupled with a simulator are developed to mimic how transport agency learns from historical data and generates traffic forecast. Properties of such a learning model are also analyzed and discussed. Impacts of adopting inaccurate parameters for the transport agency have been examined numerically. Note that the learning and simulating framework developed in this paper might be further integrated into a detailed simulation for large-scale networks in the future (e.g., Hu and Mahmassani, 1997).

The rest of the paper is organized as follows. Section 2 describes the bi-modal commuting problem, provides cost formulations for travelers, and revisits the bi-modal user equilibrium. In Section 3, the day-to-day learning behaviors of the travelers and the traffic information agency are modeled and illustrated. Section 4 numerically illustrates the dynamic traffic evolution and verifies the applicability of the proposed model. Particularly, impacts of traffic forecast and user inertia are examined and a sensitivity analysis regarding a number of key parameters in the paper is conducted. Finally, Section 5 concludes the paper.

2 Formulation for User Equilibrium

We start with a thumbnail description of the rush-hour commuting problem with both departure time and travel mode choice, and then formulate the travel costs of different modes and revisit the bi-modal commuting equilibrium. Detailed mathematical derivations for the user

equilibrium solutions are omitted as they have been well studied in the literature mentioned in Section 1.

We consider the city transportation network in Figure 1, where there is a highway and a parallel public transit line (with dedicated right-of-way) connecting home and the workplace (i.e., central business district or CBD). There is a highway bottleneck with fixed capacity that is located between home and workplace (along the highway). Travelers can either drive through the highway or take the public transit to work. The total number of travelers N is fixed, and $N = N_a + N_b$, where N_a and N_b represent the numbers of auto and transit users, respectively. Note that we use the subscript “ b ” rather than “ t ” to refer to the public transit, which is to avoid confusion with the notation for time t later.

“place Figure 1 about here”

We now describe the auto commuting trips through the bottleneck-constrained road. Auto commuters (those drive to work) have to make a trade-off between the travel time cost dependent on the queue length experienced at the highway bottleneck and the schedule delay cost associated with arriving early or late at work. The total travel cost of a traveler departing at time t is the sum of travel time cost and schedule delay cost, which is given by

$$c_a(t) = \alpha \cdot T(t) + \beta \cdot \max\{0, t^* - t - T(t)\} + \gamma \cdot \max\{0, t + T(t) - t^*\}, \quad (1)$$

where α is value of time (VOT), β and γ are the early and late arrival penalties (for a unit of time) respectively, $T(t)$ is the travel time for travelers departing at time t , and t^* is the desired arrival time at work. It is assumed that $\gamma > \alpha > \beta$, which is consistent with empirical evidences. Moreover, without loss of generality, we assume that the travel time $T(t)$ only contains the queuing delay, i.e., $T(t) = q(t)/s$, where $q(t)$ is the (point) queue, and s is the highway bottleneck capacity.

At the departure/arrival equilibrium, the departure rates from home (or arrival rates at the highway bottleneck) of those arriving at work early and late are respectively

$$\frac{\alpha}{\alpha - \beta}s; \frac{\alpha}{\alpha + \gamma}s. \quad (2)$$

When the total number of auto commuter is N_a , the morning peak begins at time $t^* - \frac{\gamma}{\beta + \gamma} \frac{N_a}{s}$

and ends at time $t^* + \frac{\beta}{\beta+\gamma} \frac{N_a}{s}$, the equilibrium departure rate of travelers from home is

$$r^*(t) = \begin{cases} 0 & t < t^* - \frac{\gamma}{\beta+\gamma} \frac{N_a}{s} \\ \frac{\alpha}{\alpha-\beta} S & t^* - \frac{\gamma}{\beta+\gamma} \frac{N_a}{s} \leq t \leq t^* - \frac{\beta}{\alpha} \frac{\gamma}{\beta+\gamma} \frac{N_a}{s} \\ \frac{\alpha}{\alpha+\gamma} S & t^* - \frac{\beta}{\alpha} \frac{\gamma}{\beta+\gamma} \frac{N_a}{s} < t \leq t^* + \frac{\beta}{\beta+\gamma} \frac{N_a}{s} \\ 0 & t > t^* + \frac{\beta}{\beta+\gamma} \frac{N_a}{s} \end{cases}, \quad (3)$$

and the equilibrium travel cost is $p_a = \frac{\beta\gamma}{\beta+\gamma} \cdot \frac{N_a}{s}$. These results are standard in the literature, one may refer to [Arnott et al. \(1990\)](#).

We now turn to the public transit commuters. The travel cost of using public transit p_b is captured by a strictly increasing function of the number of transit commuters, i.e., $p_b = c_b(N_b)$, where $c_b(\cdot)$ is the transit cost function.¹ This increasing function (over the number of users) can reflect the crowding effect in the public transit. An alternative interpretation is that this cost function is a reduced form of the model in which transit users make time-of-use decisions as well and are subject to schedule delay costs, see e.g., [Kraus \(2003\)](#). The above formulations indicate that we do not model time-dependent services in the transit side. Similar treatment can be found in e.g., [Tabuchi \(1993\)](#); [Zhang et al. \(2011\)](#). This treatment helps to reduce the complexity to simultaneously consider departure time and mode choices in a day-to-day context, i.e., when travelers shift from auto to transit, there is no departure time dimension in the transit side to consider. Future research might consider time-dependent transit service as well as transit services that are responsive to roadway network conditions (e.g., [Zhang et al., 2014, 2016](#)).

Let $[0, L]$ denote the modeling duration (which is longer than the peak duration) and $t \in [0, L]$. The set of the feasible departure rates of auto mode and the public transit flow can be written as follows:

$$\Omega \equiv \left\{ r(t), N_b, t \in [0, L] \left| \int_0^L r(t) dt = N_a, N_a + N_b = N, r(t) \geq 0, N_b \geq 0 \right. \right\}. \quad (4)$$

At the bi-modal commuting equilibrium (interior equilibrium is assumed where both auto and transit modes are used by some travelers), we should have $p_a = p_b$ and $N_a + N_b = N$. And

¹If we explicitly model the transit fare *fare*, the transit headway *headway*, the transit travel time *time*, and the transit crowding cost *crowd* in this paper, the transit cost function can be written as $c_b(N_b) = \alpha \cdot (0.5 \cdot \text{headway} + \text{time}) + \text{fare} + \text{crowd}$, where *crowd* is an increasing function of $\text{time} \cdot N_b$. This cost formulation is adopted in many studies ([Wu and Huang, 2014](#); [Wang et al., 2017](#)). Note that since we do not consider time-dependent transit services (i.e., we have constant transit headway, fare, transit travel time) in the paper, the reduced form adopted is sufficient to capture the major feature (transit cost increases over the number of users) of the more detailed transit cost formulation mentioned here.

the auto departure rates are given in Eq.(3). As the auto cost p_a monotonically increases with N_a and the transit cost p_b monotonically increases with N_b , the bi-modal user equilibrium solution is unique. For the uniqueness of the departure/arrival equilibrium for auto travelers at the highway bottleneck, one may refer to Lindsey (2004). Note that if non-zero auto free-flow time is considered in the paper, then the interior equilibrium assumption indicates that $\alpha \times (\text{auto free-flow time}) < c_b(N)$, which is automatically satisfied if we assume zero free-flow time.

3 Day-to-day Dynamics with Information Provision and User Inertia

In this paper, the focus is not on the bi-modal user equilibrium solution itself, but is on the evolution process towards the equilibrium. Particularly of our interest is how the information provision and user inertia might affect the day-to-day evolution of the bi-modal system traffic dynamics. This section firstly formulates the day-to-day learning of travelers from both past travel experiences and traffic forecast provided by the transport agency and the resultant traffic dynamics, and then proposes and illustrates a day-to-day learning model for the transport agency to learn from historical data and generate traffic forecast.

3.1 Day-to-Day User Learning and Traffic Dynamics

We consider a discrete-time day-to-day learning model where the calendar day is denoted by n . On a day-to-day basis, travelers update their perceived travel cost and adjust departure time and mode choices based on the perception, which is generally in line with the models of, e.g., Bie and Lo (2010). In particular, the perceived travel cost at day n for auto is denoted by $c_{a,p}^{(n)}(t)$, the experienced cost is $c_{a,e}^{(n)}(t)$, and the estimated cost based on traffic forecast provided by the transport agency is $c_{a,f}^{(n)}(t)$ (“forecast cost” hereafter). Similarly, the perceived travel cost at day n for transit is $c_{b,p}^{(n)}$, the experienced cost is $c_{b,e}^{(n)}$, and the forecast cost suggested by the transport agency is $c_{b,f}^{(n)}$. Note that we do not have the time-index t for transit costs, as transit cost is simplified as a function of the total number of transit users, which is time-independent.

For auto users, the perceived travel cost of departing at time t on day $n + 1$ is

$$c_{a,p}^{(n+1)}(t) = \eta_p \cdot c_{a,p}^{(n)}(t) + \eta_e \cdot c_{a,e}^{(n)}(t) + \eta_f \cdot (c_{a,f}^{(n+1)}(t) - c_{a,f}^{(n)}(t)), \quad (5)$$

where $\eta_p > 0$, $\eta_e > 0$, $\eta_f > 0$, and $\eta_p + \eta_e = 1$. Eq.(5) means that the travelers’ perceived

cost on day $n + 1$ is a linear combination the perceived cost and experienced cost on day n , and then plus the forecast cost difference between days $n + 1$ and n . A similar learning model was studied in [Liu and Geroliminis \(2017\)](#) where real-time traffic information rather than forecast cost is taken into account in the day-to-day learning framework, but neither departure time choice nor user inertia has been examined in their paper.

Similarly, the perceived travel cost of transit mode on day $n + 1$ can be written as

$$c_{b,p}^{(n+1)} = \eta_p \cdot c_{b,p}^{(n)} + \eta_e \cdot c_{b,e}^{(n)} + \eta_f \cdot (c_{b,f}^{(n+1)} - c_{b,f}^{(n)}). \quad (6)$$

Eq.(5) and Eq.(6) together constitute a more general modeling framework than the literature for the day-to-day user learning, which explicitly takes into account both past travel experience and the traffic forecast. This model includes those in the literature (e.g., [Bie and Lo, 2010](#)) as special cases where $\eta_f = 0$.

We now look at the flow adjustment dynamics. Auto departure rate at time t on day n is denoted by $r^{(n)}(t)$ and $\int_0^L r^{(n)}(t)dt = N_a^{(n)}$, and the total transit demand is $N_b^{(n)}$ where $N_a^{(n)} + N_b^{(n)} = N$. The proportional swap flow adjustment process is modified to capture the the departure time and mode shifts, as well as the user inertia. Particularly, the departure rate from home on day $n + 1$ at time t is

$$r^{(n+1)}(t) = r^{(n)}(t) + E^{(n+1)}(t) + F^{(n+1)}(t), \quad (7)$$

and $E^{(n+1)}(t)$ and $F^{(n+1)}(t)$ are defined as follows:

$$E^{(n+1)}(t) = \rho \cdot \int_{\max(0,t-\Delta)}^{\min(L,t+\Delta)} (r^{(n)}(u) \cdot [c_{a,p}^{(n+1)}(u) - c_{a,p}^{(n+1)}(t)]_+ - r^{(n)}(t) \cdot [c_{a,p}^{(n+1)}(t) - c_{a,p}^{(n+1)}(u)]_+) du. \quad (8)$$

$$F^{(n+1)}(t) = \mu \cdot N_b^{(n)} \cdot [c_{b,p}^{(n+1)} - c_{a,p}^{(n+1)}(t)]_+ - \nu \cdot r^{(n)}(t) \cdot [c_{a,p}^{(n+1)}(t) - c_{b,p}^{(n+1)}]_+, \quad (9)$$

where $[\cdot]_+ = \max\{0, \cdot\}$. In Eq.(7), $E^{(n+1)}(t)$ corresponds to the departure time shifting and $F^{(n+1)}(t)$ corresponds to the mode shifting of users, where ρ , μ and ν are the three adjusting coefficients. Note that, in the mode shifting adjustment, as the departure time dimension in the public transit is not considered, the total number of transit users $N_b^{(n)}$ is used rather than a transit departure rate. Moreover, in Eq.(8), Δ is introduced to reflect the user inertia when adjusting departure time, which represents the upper bound of departure time shift in a single day. It suggests that for a traveler departing at time t on day n , he or she will forward or postpone his or her departure time by no more than Δ in a single-day adjustment,

i.e., his or her departure time on day $n + 1$ should be within $[t - \Delta, t + \Delta]$. A special case is that $\Delta = +\infty$ thus the travelers may depart at any time no matter when he or she departs in the previous day. Note that the departure time is also constrained by $t \geq 0$ and $t \leq L$ as we focus on time interval $[0, L]$. The above treatment with departure time shift upper bound Δ is relevant to but different from those day-to-day models considering bounded rationality, where users may not shift their choices as long as the cost difference is within certain gap. Accordingly, the flow adjustment from day to day in the transit mode is

$$N_b^{(n+1)} = N_b^{(n)} - \int_0^L F^{(n+1)}(t)dt. \quad (10)$$

Since $\int_0^L \int_{\max(0, t-\Delta)}^{\min(L, t+\Delta)} (\cdot) du dt = \int_{\max(0, u-\Delta)}^{\min(L, u+\Delta)} \int_0^L (\cdot) du dt$ (the left and right sides of the equation integrate the same formula over the same area), it is easy to obtain $\int_0^L E^{n+1}(t)dt=0$. Hence, based on Eq.(7) and Eq.(10), $N_a^{(n)} + N_b^{(n)} = N$ for all $n = 1, 2, 3, \dots$, which means that the flow conservation condition is always respected.

The above modified proportional swap system is able to incorporate flow changes due to departure time and mode shifts and the user inertia's impacts. The adjustment parameters $\rho > 0$, $\mu > 0$, and $\nu > 0$ should be small enough so that the adjustment is gradual and fine. Note that generally $\mu \neq \nu$ should hold as the total number of transit users $N_b^{(n)}$ usually has a much larger magnitude than the departure rate $r^{(n)}(t)$.

3.2 Day to Day Traffic Forecasting of Transport Agency

The development of information and communications technology and the wide-spread use of smart-phones and connected information services have pervasive impacts on people's travel behavior. In this paper, one of the main aims is to model how the traffic forecast (forecast travel cost) provided by the transport agency can affect users' choices. Particularly, we consider that the transport agency can take advantage of historical data in updating the traffic forecast from day to day. We now describe the auxiliary learning and simulation framework for the transport agency. A flowchart to show the forecast process is displayed in Figure 2.

The first step for the transport agency is to predict the users' perceived travel cost. Specifically, the following learning model is used for the transport agency, i.e., the forecast of users' perceived cost of driving is

$$c_{a,fp}^{(n+1)}(t) = \eta'_p \cdot c_{a,fp}^{(n)}(t) + \eta'_e \cdot c_{a,e}^{(n)}(t), \quad (11)$$

and similarly, the forecast for the perceived travel cost of transit mode on day $n + 1$ is

$$c_{b,fp}^{(n+1)} = \eta'_p \cdot c_{b,fp}^{(n)} + \eta'_e \cdot c_{b,e}^{(n)}, \quad (12)$$

where $\eta'_p > 0$, $\eta'_e > 0$, and $\eta'_p + \eta'_e = 1$. Eq.(11) and Eq.(12) together mean that the transport agency updates day $(n + 1)$'s forecast of the perceived cost as a convex combination of day n 's forecast of the perceived cost and day n 's experienced cost of users (from real data). It is possible that $\eta'_p \neq \eta_p$, $\eta'_e \neq \eta_e$, which means that the transport agency does not have exact information about how travelers value long-term perception with respect to single day's experience when updating their perceptions.

“place Figure 2 about here”

Similar to the real flow adjustment, the flow forecast on day $n + 1$ is based on the realized flow of yesterday and the forecast of the perceived cost, which is given in the following. For auto departure,

$$r_f^{(n+1)}(t) = r^{(n)}(t) + E_f^{(n+1)}(t) + F_f^{(n+1)}(t), \quad (13)$$

where $E_f^{(n+1)}$ and $F_f^{(n+1)}$ are defined as

$$E_f^{(n+1)}(t) = \rho' \cdot \int_{\max(0, t-\Delta')}^{\min(L, t+\Delta')} (r^{(n)}(u) \cdot [c_{a,fp}^{(n+1)}(u) - c_{a,fp}^{(n+1)}(t)]_+ - r^{(n)}(t) \cdot [c_{a,fp}^{(n+1)}(t) - c_{a,fp}^{(n+1)}(u)]_+) du. \quad (14)$$

$$F_f^{(n+1)}(t) = \mu' \cdot N_b^{(n)} \cdot [c_{b,fp}^{(n+1)} - c_{a,fp}^{(n+1)}(t)]_+ - \nu' \cdot r^{(n)}(t) \cdot [c_{a,fp}^{(n+1)}(t) - c_{b,fp}^{(n+1)}]_+, \quad (15)$$

and the forecast flow for transit mode is

$$N_{b,f}^{(n+1)} = N_b^{(n)} - \int_0^L F_f^{(n+1)}(t) dt. \quad (16)$$

Note again that, a superscript “ ’ ” is added to distinguish ρ' , μ' , ν' and Δ' adopted by the transport agency from ρ , μ , ν , and Δ of travelers, which means that the transport agency might adopt different/inaccurate parameters for flow adjustment from the real ones. ρ' , μ' , and ν' should also be small enough so that the predicted adjustment is gradual and fine. However, as can be seen in Eqs.(13)-(16), historical information (e.g., real flows in the previous day) is assumed to be available to the transport agency and has been used in the flow prediction process. This suggests that the transport agency is “smart” which can absorb real flow information from day to day.

As shown in Figure 2, in the third step, the transport agency takes the forecast flows given in Eq.(13) and Eq.(16) as inputs for the traffic simulator which generates the predicted traffic conditions. These predicted conditions are then utilized by travelers to calculate the forecast cost for day $n + 1$, or the predicted experienced cost $c_{a,f}^{(n+1)}(t)$ based on the forecast flow. The traffic simulator adopted by the transport agency exactly simulates the bi-modal system described in Section 2, where Figure 1 displays the city network structure. In practice, when a more complicated network settings and demand patterns are in presence, a more complicated simulator should be developed and calibrated with real traffic data and relevant survey data. However, as this is not the focus of the current paper, we thus leave it for future research.

Proposition 3.1. *The transport agency's learning model for prediction satisfies the following: If $c_{a,e}^{(n+1)}(t) - c_{a,e}^{(n)}(t) = 0$ or $c_{b,e}^{(n+1)} - c_{b,e}^{(n)} = 0$ holds for any $n \geq n_0$, then $c_{a,fp}^{(n+1)}(t) \rightarrow c_{a,fp}^{(n)}(t) \rightarrow c_{a,e}^{(n_0)}(t)$ or $c_{b,fp}^{(n+1)} \rightarrow c_{b,fp}^{(n)} \rightarrow c_{b,e}^{(n_0)}$ when $n \rightarrow +\infty$.*

Proof. We take the case with $c_{a,e}^{(n+1)}(t) - c_{a,e}^{(n)}(t) = 0$ for $n \geq n_0$ as an example. Based on Eq.(11), we have

$$c_{a,fp}^{(n+1)}(t) - c_{a,e}^{(n_0)}(t) = \eta'_p \cdot c_{a,fp}^{(n)}(t) + \eta'_e \cdot c_{a,e}^{(n)}(t) - c_{a,e}^{(n_0)}(t).$$

For $n \geq n_0$, as $c_{a,e}^{(n+1)}(t) - c_{a,e}^{(n)}(t) = 0$, and $\eta'_p + \eta'_e = 1$, we further have

$$c_{a,fp}^{(n+1)}(t) - c_{a,e}^{(n_0)}(t) = \eta'_p \cdot c_{a,fp}^{(n)}(t) + \eta'_e \cdot c_{a,e}^{(n_0)}(t) - c_{a,e}^{(n_0)}(t) = \eta'_p \cdot [c_{a,fp}^{(n)}(t) - c_{a,e}^{(n_0)}(t)].$$

Therefore, for $n \geq n_0$

$$c_{a,fp}^{(n+1)}(t) - c_{a,e}^{(n_0)}(t) = (\eta'_p)^{n+1-n_0} \cdot [c_{a,fp}^{(n_0)}(t) - c_{a,e}^{(n_0)}(t)].$$

As $0 < \eta'_p < 1$, when $n \rightarrow +\infty$,

$$c_{a,fp}^{(n+1)}(t) - c_{a,e}^{(n_0)}(t) \rightarrow 0 \cdot [c_{a,fp}^{(n_0)}(t) - c_{a,e}^{(n_0)}(t)] = 0.$$

It follows that $c_{a,fp}^{(n+1)}(t) \rightarrow c_{a,fp}^{(n)}(t) \rightarrow c_{a,e}^{(n_0)}(t)$ holds when $n \rightarrow +\infty$. Similar treatments can be given for the case for $c_{b,e}^{(n+1)} - c_{b,e}^{(n)} = 0$. This completes the proof. \square

We summarize an important property of the transport agency's learning model in Proposition 3.1. It states that if the real experienced cost of the travelers remains constant from day to day, the forecast perceived cost will approach this constant value as well, indicating

that the transport agency is “smart” that it can eventually learn the the “correct” values and parameters in the transport systems.

3.3 The Stationary Point

Now we turn to discuss the stationary point of the dynamical system defined by Eq.(5)-(10). Denote the equilibrium numbers of auto and public transit commuters by N_a^* and N_b^* , respectively. At the fixed point, we should have $\mathbf{r}^{(n+1)} = \mathbf{r}^{(n)} = \mathbf{r}^* = (r^*(t), t \in [0, L])$, $N_b^{(n+1)} = N_b^{(n)} = N_b^*$; and $\mathbf{c}_{a,p}^{(n+1)} = \mathbf{c}_{a,p}^{(n)} = \mathbf{c}_{a,p}^* = (c_{a,p}^*(t), t \in [0, L])$, $c_{b,p}^{(n+1)} = c_{b,p}^{(n)} = c_{b,p}^*$. Note that departure rate profile $r^*(t)$ is given in Section 2 for those arriving earlier or later than the desired arrival time. Furthermore, we should have $\mathbf{c}_{a,f}^{(n+1)} = \mathbf{c}_{a,f}^{(n)} = \mathbf{c}_{a,f}^* = (c_{a,f}^*(t), t \in [0, L])$, $c_{b,f}^{(n+1)} = c_{b,f}^{(n)} = c_{b,f}^*$. This suggests that the third terms in the right-hand side of Eq.(5) and Eq.(6) will be zero.

It is assumed that for auto users the initial departure rate $r^{(0)}(t)$ is continuous in t for the time intervals $\left[0, t^* - \frac{\gamma}{\beta+\gamma} \frac{N_a^*}{s}\right)$, $\left[t^* - \frac{\gamma}{\beta+\gamma} \frac{N_a^*}{s}, t^* - \frac{\beta}{\alpha} \frac{\gamma}{\beta+\gamma} \frac{N_a^*}{s}\right]$, $\left(t^* - \frac{\beta}{\alpha} \frac{\gamma}{\beta+\gamma} \frac{N_a^*}{s}, t^* + \frac{\beta}{\beta+\gamma} \frac{N_a^*}{s}\right]$, and $\left(t^* + \frac{\beta}{\beta+\gamma} \frac{N_a^*}{s}, L\right]$. Besides, the initial forecast of users perceived travel cost $c_{a,fp}^{(0)}(t)$ and initial perceived travel cost $c_{a,p}^{(0)}(t)$ are assumed to be continuous during the time interval $[0, L]$. With these assumptions, the following result regarding the stationary point can be established.

Proposition 3.2. *Suppose (1) the initial auto departure rate $r^{(0)}(t)$ is continuous in t for the time intervals $\left[0, t^* - \frac{\gamma}{\beta+\gamma} \frac{N_a^*}{s}\right)$, $\left[t^* - \frac{\gamma}{\beta+\gamma} \frac{N_a^*}{s}, t^* - \frac{\beta}{\alpha} \frac{\gamma}{\beta+\gamma} \frac{N_a^*}{s}\right]$, $\left(t^* - \frac{\beta}{\alpha} \frac{\gamma}{\beta+\gamma} \frac{N_a^*}{s}, t^* + \frac{\beta}{\beta+\gamma} \frac{N_a^*}{s}\right]$, and $\left(t^* + \frac{\beta}{\beta+\gamma} \frac{N_a^*}{s}, L\right]$, and (2) the initial forecast of users’ perceived travel cost $c_{a,fp}^{(0)}(t)$ and the initial perceived travel cost $c_{a,p}^{(0)}(t)$ are continuous during the time interval $[0, L]$, the dynamical system Eq.(5)-(10) has a unique stationary point which coincides with the static equilibrium solution where Eq.(3) holds and $c_a(t) = c_b(N_b^*)$ for $t \in \left[t^* - \frac{\gamma}{\beta+\gamma} \frac{N_a^*}{s}, t^* + \frac{\beta}{\beta+\gamma} \frac{N_a^*}{s}\right]$.*

Proof. For presentation purpose, we use t_q^* , t_q^* , and t_o^* to represent $t^* - \frac{\gamma}{\beta+\gamma} \frac{N_a^*}{s}$, $t^* + \frac{\beta}{\beta+\gamma} \frac{N_a^*}{s}$ and $t^* - \frac{\beta}{\alpha} \frac{\gamma}{\beta+\gamma} \frac{N_a^*}{s}$, respectively.

Since it is assumed that for auto users the initial departure rate $r^{(0)}(t)$ is continuous in t over the intervals $[0, t_q^*]$, $[t_q^*, t_o^*]$, $(t_o^*, t_q^*]$ and $(t_q^*, L]$, according to Guo et al. (2017a) and Theorems 3.2.8 and 3.3.9 in Trench (2013), $r^{(0)}(t)$ is integrable and $c_{a,e}^{(0)}(t)$ is continuous over $[0, L]$.

Also since $c_{a,fp}^{(0)}(t)$ is continuous over $[0, L]$, based on Eq.(11), we have $c_{a,fp}^{(1)}(t)$ to be continuous over $[0, L]$. Then, from Eq.(13) to Eq.(15) and the definition of $c_{a,f}^{(1)}(t)$, it can be obtained that $r_f^{(1)}(t)$ is continuous in t on the intervals $[0, t_q^*]$, $[t_q^*, t_o^*]$, $(t_o^*, t_q^*]$ and $(t_q^*, L]$

and $c_{a,f}^{(1)}(t)$ is continuous on $[0, L]$. As a result, $c_{a,p}^{(1)}(t)$ is continuous on $[0, L]$, given Eq.(5) and the assumption that $c_{a,p}^{(0)}(t)$ is continuous on $[0, L]$. Following Eqs.(7)-(9) we can also obtain that $r^{(1)}(t)$ is continuous in t on the intervals $[0, t_q^*], [t_q^*, t_o^*], (t_o^*, t_{q'}^*]$ and $(t_{q'}^*, L]$. Consequently, the auto departure rate $r^{(n)}(t)$ is continuous in t on the intervals $[0, t_q^*], [t_q^*, t_o^*], (t_o^*, t_{q'}^*]$ and $(t_{q'}^*, L]$, the forecast of auto users' perceived travel cost $c_{a,fp}^{(n)}(t)$ and the perceived travel cost $c_{a,p}^{(n)}(t)$ are continuous over $[0, L]$ at any iteration/day n .

At the stationary point $r^{(n+1)}(t) = r^{(n)}(t) = r^{(n-1)}(t) = r^*(t)$, $N_b^{(n+1)} = N_b^{(n)} = N_b^{(n-1)} = N_b^*$, then the experienced costs of each mode at the stationary point satisfy $c_{a,e}^{(n+1)}(t) = c_{a,e}^{(n)}(t) = c_{a,e}^*(t)$ and $c_{b,e}^{(n+1)} = c_{b,e}^{(n)} = c_{b,e}^* = c_b(N_b^*)$. According to Proposition 3.1, we have $c_{a,fp}^{(n+1)}(t) = c_{a,fp}^{(n)}(t)$ and $c_{b,fp}^{(n+1)} = c_{b,fp}^{(n)}$. Based on Eqs.(13)-(16), we have $r_f^{(n+1)}(t) = r_f^{(n)}(t)$ and $N_{b,f}^{(n+1)} = N_{b,f}^{(n)}$. Hence, $c_{a,f}^{(n+1)}(t) = c_{a,f}^{(n)}(t)$ and $c_{b,f}^{(n+1)} = c_{b,f}^{(n)}$. It follows from Eq.(5) that $\mathbf{c}_{a,p}^* = \mathbf{c}_{a,e}(\mathbf{r}^*) = (c_{a,e}^*(t), t \in [0, L])$ and $c_{b,p}^* = c_b(N_b^*) = c_{b,e}^*$. Then the stationary point is the solution of Eq.(17)

$$\begin{cases} r^*(t) = r^*(t) + E^*(t) + F^*(t) \text{ for } t \in [0, L] \\ N_b^* = N_b^* - \int_0^L F^*(t) dt \end{cases}, \quad (17)$$

where

$$E^*(t) = \rho \int_{\max(0, t-\Delta)}^{\min(L, t+\Delta)} \left(r^*(u) [c_{a,e}^*(u) - c_{a,e}^*(t)]_+ - r^*(t) [c_{a,e}^*(t) - c_{a,e}^*(u)]_+ \right) dt, \quad (18)$$

and

$$F^*(t) = \mu \cdot N_b^* \cdot [c_{b,e}^* - c_{a,e}^*(t)]_+ - \nu \cdot r^*(t) \cdot [c_{a,e}^*(t) - c_{b,e}^*]_+. \quad (19)$$

Then all the preconditions of Corollary 1 in Guo et al. (2017b) are satisfied. Following the proofs of Theorem 1 and Corollary 1 in Guo et al. (2017b), it can be shown that the function $F: \mathbf{r}^* \rightarrow \mathbf{r}^* + \mathbf{E}^*(\mathbf{r}^*) + \mathbf{F}^*(\mathbf{r}^*)$, $N_b^* \rightarrow N_b^* - \int_0^L F^*(t) dt$ is continuous on set Ω and maps Ω to itself. Moreover, the set Ω is nonempty, convex and compact. Thus, according to Brouwer's existence theorem, there exists at least one stationary solution(s).

Obviously, the deterministic user equilibrium solution as in Eq.(3) where $c_a(t) = c_b(N_b)$ for $[t_q^*, t_{q'}^*]$ with $r(t) > 0$ is a stationary point of the dynamical system. Suppose there is another (different) stationary point, then there exists a time t' that satisfies $c_b(N_b^*) - c_{a,e}^*(t') \neq 0$ with $r^*(t') > 0$. Without loss of generality, it is supposed that $c_{a,e}^*(t') > c_b(N_b^*)$ and $t' = \arg \max_{t \in [0, L]} c_{a,e}^*(t)$. Then $E^*(t') \leq 0$ and $F^*(t') < 0$, which contradicts the equation $r^*(t') = r^*(t') + E^*(t') + F^*(t')$. Thus, the stationary point must coincide with the bi-modal user equilibrium solution, which is unique as discussed in Section 2. \square

The stability of the stationary point is extremely difficult to analyze analytically if not impossible. This is because that the auto travel cost is not always differentiable (due to the piece-wise linear schedule delay cost functions) and is asymmetric (due to the asymmetric impacts of the flows at different departure times on travel cost). To explore the the stability of the stationary point and the impact of different values of η_f on the stability, we have made a few simplifying assumptions, and presented some theoretical analysis in Appendix A.1.

4 Numerical Experiments

This section presents some numerical experiments to illustrate the proposed model. Particularly, we firstly describe the discretization of time and list the benchmark numerical settings for the numerical analysis. Then, we explore the day-to-day evolution process of the traffic dynamics in the bi-modal system, and examine its convergence to the user equilibrium solution. Finally, we conduct a series of sensitivity analysis to explore the impacts of a number of parameters in the day-to-day model and explain the implications. We start with summarizing the basic numerical setting in Table 1.

“place Table 1 about here”

In the numerical analysis, the time horizon $[0, L]$ is discretized into M time intervals for each day, and the length of each interval is $l = 1(\text{min})$ so that $M \cdot l = L$. Specifically, we let $L = 2$ (hours), and thus $M = 120$. Besides, $t^* = 0.6 \cdot (L - 0) = 1.2$ (hour). Also note that in the later analysis, we adopt an upper bound for departure time shifting Δ of 60 minutes, and as l is 1 minute, we have $\delta = 60$ (note that for a smaller l , we have a larger δ). Moreover, if we do not specify the detailed setting, we let $\Delta' = \Delta$.

According to this discretized timeline, we can derive the discrete version of the travel costs, and the day-to-day flow adjustment. The auto cost of the traveler departing at time step i is

$$c_a(i) = \alpha \cdot T(i) + \beta \cdot \max\{0, t^* - (i - 1) \cdot l - T(i)\} + \gamma \cdot \max\{0, (i - 1) \cdot l + T(i) - t^*\}, \quad (20)$$

where $i = 1, 2, 3, \dots, M$. Travel time for this traveler is $T(i) = q(i)/s$ where $q(i)$ is the queue length. Similarly, the perceived cost, experienced cost, forecast cost, and forecast perceived cost for given mode and given day are converted into discrete forms $c_{mode,indicator}^{(n)}(i)$, where $mode = a, b$, $indicator = p, e, f, fp$, and again n is the day index, and i is the time step. Note that for the discrete version of the model, we simply adopt the same notation while we replace time index t by time step index i to avoid additional notation burden.

The discrete form of the flow adjustment process can be similarly given by

$$r^{(n+1)}(i) = r^{(n)}(i) + E^{(n+1)}(i) + F^{(n+1)}(i), \quad (21)$$

and $E^{(n+1)}(i)$ is defined as:

$$E^{(n+1)}(i) = l \cdot \rho \cdot \sum_{j=\max(1, i-\delta)}^{\min(M, i+\delta)} (r^{(n)}(j)[c_{a,fp}^{(n+1)}(j) - c_{a,fp}^{(n)}(j)]_+ - r^{(n)}(i)[c_{a,fp}^{(n+1)}(i) - c_{a,fp}^{(n)}(i)]_+), \quad (22)$$

where δ is an integer, and $\Delta = l \cdot \delta$; and $F^{(n+1)}(i)$ is defined as:

$$F^{(n+1)}(i) = l \cdot \left[\mu \cdot N_b^{(n)} \cdot \left[c_{b,p}^{(n+1)} - c_{a,p}^{(n+1)}(i) \right]_+ - \nu \cdot r^{(n)}(i) \cdot \left[c_{a,p}^{(n+1)}(i) - c_{b,p}^{(n+1)} \right]_+ \right] \quad (23)$$

The flow adjustment for transit mode can then be written as

$$N_b^{(n+1)} = N_b^{(n)} - \sum_{i=1}^M F^{(n+1)}(i). \quad (24)$$

The formulas associated with the transport agency in Eqs.(11)-(16) can be converted to the discrete forms analogously, of which the details are omitted.

We also define the following error term for the system to identify if the system reaches the bi-modal commuting equilibrium.

$$\epsilon^{(n)} = \sum_{i=1}^M \left[\frac{r^{(n)}(i)}{N} |c_{a,e}^{(n)}(i) - c_{ave}^{(n)}| \right] + \frac{N_t^{(n)}}{N} |c_{b,e}^{(n)} - c_{ave}^{(n)}|, \quad (25)$$

where $c_{ave}^{(n)} = \sum_{i=1}^M \left[\frac{r^{(n)}(i)}{N} c_{a,e}^{(n)}(i) \right] + \frac{N_t^{(n)}}{N} c_{b,e}^{(n)}$ represents the average cost among all users. When the system approaches the dynamic user equilibrium solution, all travelers' costs approach this same value, and thus $\epsilon^{(n)}$ in Eq.(25) will be close to zero.

4.1 Convergence to User Equilibrium

This subsection mainly illustrates the convergence of the day-to-day evolution process to the user equilibrium. Figure 3 shows the evolution of perceived travel costs, experienced travel costs of auto users departing at three different times (representative individuals choosing departure time 40/60/80 min) and these costs of the users taking transit. It also shows the evolution of the forecast perceived costs and the derived forecast cost provided by transport agency of different modes and departure times. As can be seen, all these costs evolve to the

same value over calendar time, suggesting that 1) the system is approaching the bi-modal dynamic user equilibrium; 2) the forecast from the transport agency approaches the real value over time.

“place Figure 3 about here”

Panel (a) in Figure 4 further shows the evolution of different types of costs for departing at 60 min. Note that the travelers departing at the same time might be different in different days. Panel (b) in Figure 4 then illustrates that the perceived cost and experienced cost of the transit travelers will approach the same value over days, and the forecast from the transport agency will also approach the real value. Moreover, these different types of costs while fluctuate over days in the beginning, they are close to each other, which is due to the interdependent relationships among them.

“place Figure 4 about here”

The traffic conditions on several representative days (Days 1, 3, 5, 7, 20, 30, 50, 150, and 500) are picked up by Figure 5 and Figure 6, showing the time-varying queue pattern at the highway bottleneck and the departure-time-based experienced travel cost of users. While only one case initiated from a particular flow pattern at day one is presented here, two other typical cases are provided in Appendix A.2 (we indeed tested many more initial flow solutions but only showed the three representative ones). As one may see, the initial flow solution in Figure 5 leads to no queue. However, as the travelers can shift to the middle of the 2 hours’ modeling period to reduce cost, queue formats over iterations, and finally approaches the triangular shape, which is the equilibrium pattern that has been well studied in the literature. Figure 6 then shows the corresponding evolution of the experienced cost over departure time. Note that in the end (Day 500), no commuter departs before approximately $t = 0.5$ hour and after approximately $t = 1.5$ hour, as the cost is larger than the equilibrium cost (which corresponds to the flat line in the middle of the 2 hours’ duration).

“place Figure 5 about here”

“place Figure 6 about here”

Those illustrated in Figure 5 and Figure 6 are not yet the full picture. Indeed, the total number of users traveling by auto is fluctuating over days as well (so is the total number of transit users). Figure 7 then presents the market share of auto mode for the whole day and the error term defined in Eq.(25) over days. It further verifies that the system approaches

the bi-modal dynamic user equilibrium over calendar time. Moreover, Figure 8 shows how the mode share evolves from different initial modal-split fractions (0.00, 0.25, 0.50, 0.75, 1.00) and converges to the identical value under the bi-modal user equilibrium solution.

“place Figure 7 about here”

“place Figure 8 about here”

Moreover, for different lengths of time step in the discretizations of clock time, i.e., l changes from 1.0 (*min*) (the benchmark value) to 0.5 (*min*), and then to 0.2 (*min*), we examine the evolution of aggregate modal-split and the error term defined in Eq.(25) over days in Figure 9. As can be seen, as l decreases, the convergence speed of the system to the bi-modal user equilibrium is smaller. Given these results, we conjecture that the day-to-day dynamical system with a continuous (within-day) time model for a single day, i.e., $l \rightarrow 0$, may have a lower convergence speed towards user equilibrium. However, this issue should be carefully and more comprehensively re-examined and theoretically analyzed, which is of our interest for future research.

“place Figure 9 about here”

Now we turn to look at the transport agency and its forecast model. Figure 10 shows the gap between the forecast flow from the agency and the realized flow in the same day. Specifically, Figure 10a shows the cumulative distribution (CDF) of $(r(t) - r_f(t))$ for some particular days (day 5, 10, 50, 100, 200, 500). As can be seen, over days the CDF curve moves towards the y-axis (i.e., line $x=0$) suggesting the discrepancy goes to zero. Figure 10b shows the corresponding mean values and standard deviations (Std) of $(r(t) - r_f(t))$ over calendar time. The standard deviation decreases over days and approaches zero in the end. These results indicate that with our learning model for the agency, the accuracy of traffic forecast is improving over time and the forecast is approaching the realized or experienced value. This also indirectly verifies Proposition 3.1.

“place Figure 10 about here”

4.2 Sensitivity Analysis

In this subsection, we explore how variations of different factors/parameters or inaccurate parameters adopted by the transport agency might affect the system dynamics and convergence.

Firstly, Figure 11 shows the evolution of modal-splits and error terms under different η_f (other parameters remain the same as in Section 4.1). When η_f decreases from 1.0 to 0.1, the convergence speed decreases (the error term is larger given the same number of iterations). And if η_f further decreases, the system does not necessarily converge to an equilibrium state (see cases with $\eta_f = 0.1$ and $\eta_f = 0.02$), and the discrepancy from the equilibrium solution becomes larger and fluctuates over calendar time. This suggests that with no or little information (or the users do not value the forecast), the system may vary from day to day and never converge to an equilibrium state. The implication is that appropriate information provision (forecast cost) could help the user behaviors and traffic dynamics in the bi-modal system to stabilize. It is also worth mentioning that a too small η_f can be interpreted as inaccurate information provision (which is then perceived by traveler). These results then indicate that inaccurate forecast might lead to non-convergence to equilibrium of the bi-modal system (this is more comprehensively discussed in Li et al. (2017)).

Guo et al. (2017a) provided an important result that traditional algorithms similar to the proportional swap system may not really solve the dynamic user equilibrium. Our results here are consistent with that (see if $\eta_f = 0.1$ and $\eta_f = 0.02$). Beyond these, our result implies that an appropriately modified system with the so-called forecast cost term might help compute the dynamic user equilibrium solution. Note that these findings are based on the discrete time day-to-day model setting. Our future research will further examine this issue theoretically.

“place Figure 11 about here”

“place Figure 12 about here”

Figure 12 further shows the system performance measures (total cost of auto travelers, total cost of transit travelers, and total cost of all travelers) over calendar time under different values of η_f (we only show the first 50 days as later these measures for different η_f converge to very similar values). For the total auto cost and total transit cost, one may notice that the fluctuations for cases with smaller η_f (0.1 or 0.02) are larger (these two terms are fluctuating in an opposite way), this is consistent with the observations in Figure 11 where the system under smaller η_f fluctuates and may not converge. However, fluctuation in total travel cost (the summation of auto cost and transit cost) is not larger, because the fluctuations in total auto and transit costs are in opposite directions. It is also worth mentioning that on average (over calendar time for the first 50 days), the cases with larger η_f have smaller total cost. This means that appropriate information provision might make the system better off. However, after the first 50 days, even the system traffic under small η_f might not

fully converge to the user equilibrium state, it can be very close to that, thus the system performance measures also become similar, and information provision becomes much less relevant to system performance.

We now turn to explore the impacts of user inertia. Figure 13 displays the evolution of modal-split and error term when different levels of user inertia prevails ($\delta = +\infty, 30, 5$). Despite the minor difference in modal-split, it is evident that the error term is larger when δ is smaller given the same number of iterations. This means that when users are more reluctant to change, i.e., δ is smaller, the system converges more slowly. In this sense, user inertia leads to ineffective system variation and slows down convergence of non-equilibrium state to the equilibrium state in the system. However, if the system is already in an equilibrium state, then user inertia help the system to stay at the equilibrium and it alleviates system variations.

“place Figure 13 about here”

In the following, we further look at the impacts of the learning parameters. Specifically, Figure 14 and Figure 15 display the evolution of modal-splits and error terms with $\eta_p \neq \eta'_p$ and $\eta_p = \eta'_p$ respectively. The three cases in Figure 14 ($\eta_p \neq \eta'_p$) suggest that even if the transport agency adopts an underestimated η_p with respect to the real value, the system is still able to converge to the equilibrium with similar convergence speed, while overestimation of η_p can lead to non-convergence. Note that a larger η'_p means a smaller η_e' . This result indicates that for the transport agency, if a smaller weight (smaller η_e') is put on most updated experienced conditions when updating its forecast, its positive impact in helping the system to stabilize decreases.

Figure 15 further displays the cases when $\eta_p = \eta'_p$ but its value varies. It shows that a larger η_p (or η'_p) results in slower convergence ($0.5 > 0.3 > 0.1$), or even non-convergence (the case with $\eta_p = \eta'_p = 0.7$). This is explained in the following. A larger η_p (as well as η'_p) implies that every individual puts more weight on long-term perception and less on yesterday’s single-day experience. The aggregate effect is that the system absorbs most updated inputs more slowly, and is more reluctant to change, and thus converges more slowly, or even does not converge.

“place Figure 14 about here”

“place Figure 15 about here”

Finally, we consider the effects of parameters characterizing the day-to-day flow adjustment process. Figure 16 and Figure 17 show the evolution of modal-splits and error terms

for the cases with $\rho' \neq \rho$, $\mu' \neq \mu$, and $\nu' \neq \nu$, or the cases with $\rho' = \rho$, $\mu' = \mu$, and $\nu' = \nu$ respectively. When transport agency adopts inaccurate parameters, i.e., $\rho' \neq \rho$, $\mu' \neq \mu$, and $\nu' \neq \nu$, either certain level of underestimation or overestimation, the system still converges to the equilibrium with very similar convergence speed, which is shown in Figure 16.

“place Figure 16 about here”

Figure 17 shows that larger values of ρ' ($= \rho$), μ' ($= \mu$) and ν' ($= \nu$) tend to result in a faster convergence speed toward user equilibrium. This is because that a larger ρ' ($= \rho$) or μ' ($= \mu$) or ν' ($= \nu$) allows larger flow adjustments between two adjacent days, and the system could change more quickly to the user equilibrium. However, when we have relatively large ρ' ($= \rho$), μ' ($= \mu$), and ν' ($= \nu$), the system may still converge, but in a fluctuating way due to non-gradual flow adjustment (see the red solid line in Figure 17). While we do not show the results, extremely large values of ρ' ($= \rho$), μ' ($= \mu$), and ν' ($= \nu$) will lead to non-convergence as the system may always have large traffic variations. Generally, these parameters have to be small enough so that the flow adjustment is gradual, and the flows will not be negative (Smith and Wisten, 1995).

“place Figure 17 about here”

5 Conclusion

This study proposes a novel framework for day-to-day evolution of both departure time choice and mode choice in a bi-modal transportation system. A day-to-day learning model for users is developed to take into account impacts of traffic forecast and user inertia on their travel choices. An auxiliary learning model coupled with a simulator has been developed to mimic how transport agency learns from historical data and generates traffic forecast. It is also shown that the proposed dynamical system has a unique stationary point which is exactly the bi-modal equilibrium solution. We also analyze the stability of the stationary point under several simplifying assumptions.

Numerical experiments further illustrate that the convergence of the proposed dynamical system is generally robust to parameter value variations and initial flow patterns. The traffic flow and travel cost forecasts, generated from the learning and simulation framework developed for the transport agency, well suited the realized values, even if some of the parameters adopted might be inaccurate. Through sensitivity analysis, we have credited the contribution of traffic information in helping or speeding system convergence by showing that with no or little information, the system is likely to vary from day to day and is unable

to converge to an equilibrium state. Also, information provision might help reduce variations in system performance over days when an equilibrium state has not been reached yet. But it is worth mentioning that inaccurate information provision might lead to non-convergence to equilibrium of the bi-modal system. Furthermore, it is found that under user inertia users are more reluctant to change, and the system converges more slowly. Lastly, it is worth mentioning that this study not only sheds light on modeling doubly dynamical systems, but also provides insights into computing the multi-modal dynamic user equilibrium.

As a first step to understand the day-to-day variation of departure time choice and mode choice, this paper has focused on simple network settings, i.e., single origin-destination pair and bottleneck-constrained road. These simplifications help to reduce complexity of the models and better understand the models and results. One of the future direction is to incorporate multiple origin-destination pairs, similar to [Liu and Geroliminis \(2017\)](#). In that case, travelers from different origin-destination pairs may interact with each other in the dynamic traffic network. Efforts should then be made to explore how these interactions would further affect the overall bi-modal system dynamics.

Besides, this study is based on deterministic user equilibrium (DUE) and deterministic choice behavior. While this approach has attracted many attentions, to further increase the applicability of the modeling framework, stochastic user equilibrium, boundedly rational user equilibrium, or mixed equilibrium, and different choice models might have been used (e.g., [Watling, 1999](#); [Huang et al., 2008](#); [Guo et al., 2017b](#); [Liu and Geroliminis, 2017](#); [Zhou et al., 2017](#)). A discussion for equilibrium in transportation network can be found in [Dixit and Denant-Boemont \(2014\)](#). Future research not only could further model the bi-modal doubly dynamics based on a non-deterministic approach, but also could collect data to analyze the equilibrium or non-equilibrium in transportation in a day-to-day variation context.

Acknowledgment. We would like to thank the anonymous referees for their constructive comments, which have helped improve an earlier version of this paper. The work described in this paper was partially supported by a grant from Hong Kong Research Grants Council (HKUST16205715). Dr. Wei Liu would like to thank the Principal’s Early Career Mobility Fund in the University of Glasgow, UK.

A Appendix

A.1 Stability of the bi-modal dynamical system and the impact of the information provision

As mentioned earlier, the stability of the stationary point of the dynamical system described in the paper is very difficult (if not impossible) to analyze due to that the experienced travel cost might not be differentiable over the flow rates (departure rates) at different times and is asymmetric. We now explore and illustrate the stability of the dynamical system with several simplifying assumptions. While we do not directly analyze the exact modeling framework in the paper, we believe that it still offers some insights on how the information provision or forecast cost might play a role in affecting system traffic dynamics.

The analysis is based on a discrete-time dynamical model and without loss of generality, we restrict the (within-day) time horizon to the peak duration $\left[t^* - \frac{\gamma}{\beta+\gamma} \frac{N_a^*}{s}, t^* + \frac{\beta}{\beta+\gamma} \frac{N_a^*}{s} \right]$, where N_a^* is the number of auto travelers at the bi-modal equilibrium. Then we discretize the time horizon into M time slices with the same length. The length of each slice is again denoted by l , i.e., $M \cdot l = \frac{N_a^*}{s}$. The value of l can be chosen to be small enough to make the discrete-time system to approximate the continuous-time model. In each time slice the departure rate is constant. Let $\mathbf{f} = (f_i, i = 1, 2, \dots, M)^M$ be the auto departure flow vector with $f_i = r(i), (i = 1, 2, \dots, M)$ being the auto departure flow in time slice i and define $\bar{\mathbf{f}} = (\mathbf{f}, N_b)^{M+1}$ as the flow vector of the bi-modal network. Then the flow feasible set can be written as $\bar{\Omega} \equiv \left\{ \bar{\mathbf{f}} \mid \sum_{i=1}^M f_i + N_b = N \right\}$. Define $c_{a,e,i}(\mathbf{f})$ as the experienced travel cost by auto commuters departing in the i^{th} time slice and $c_{b,e}(N_b)$ as the experienced cost for transit commuters, then $\mathbf{c}_{a,e}(\mathbf{f}) = \{c_{a,e,1}(\mathbf{f}), c_{a,e,2}(\mathbf{f}), \dots, c_{a,e,M}(\mathbf{f})\}^M$, $\mathbf{c}(\bar{\mathbf{f}}) = \{\mathbf{c}_{a,e}(\mathbf{f}), c_{b,e}(N_b)\}^{M+1}$. We further make the following assumptions to enable analytical derivations.

Assumption 1. *The experienced auto travel cost of departing in the i^{th} time slice is only related to the auto flows departing before and in this time, i.e., $c_{a,e,i}(\mathbf{f}) = c_{a,e,i}(f_1, f_2, \dots, f_i)$ and $c_{a,e,i}(\mathbf{f})$ is strictly positive derivable with respect to \mathbf{f} .*

In the bottleneck model, the experienced auto travel cost is not derivable with respect to \mathbf{f} . We make this assumption to allow for derivations when we explore the impact of different η_f values on the stability of the bi-modal dynamical system. However, the travel cost structure in the above still mimics the case with the bottleneck model where later departure would not affect travel cost of users departing earlier but earlier departure might affect travel cost of users departing later.

Assumption 2. *The forecast travel cost based on transport agency's information provision is linear positive related to the travelers' experienced travel cost, i.e., $c_{a,f,i} = \kappa \cdot c_{a,e,i}$ and $\kappa > 0$.*

This assumption allows us to have a simple analytical form for the forecast cost. When $\kappa = 1$, it means that forecast cost is perfectly accurate. As already discussed in the paper, the forecast cost is based on another level of learning and simulation, which further complicates the dynamical system. We will explore this issue in our future study. The current simplifying assumption can be reasonable as one may realize from the numerical experiments in Section 4, such as those in Figure 3 and Figure 4, that the two costs (forecast cost and experienced cost) exhibit strong positive relationships.

Before moving further, we define $\omega = \eta_f \cdot \kappa > 0$, then Eq.(5) and Eq.(6) can be rewritten as:

$$c_{a,p,i}^{(n+1)} = (\eta_e - \omega) c_{a,e,i}(\mathbf{f}^{(n)}) + (1 - \eta_e) c_{a,p,i}^{(n)} + \omega c_{a,e,i}(\mathbf{f}^{(n+1)}), \quad \text{for } i = 1, 2, \dots, M \quad (26)$$

and

$$c_{b,p}^{(n+1)} = (\eta_e - \omega) c_{b,e}(N_b^{(n)}) + (1 - \eta_e) c_{b,p}^{(n)} + \omega c_{b,e}(N_b^{(n+1)}). \quad (27)$$

We then can analyze how the parameter ω could affect the stability. Note that if we assume $\kappa = 1$ (forecast is accurate), then we have $\eta_f = \omega$. Besides, we have the following assumptions to simplify the flow adjustment process, which help to reduce complexity in capturing the flow dynamics.

Assumption 3. *Departure time shifting is negligible, i.e., $\rho=0$ or $\Delta=0$ and the flow swapping rate is constantly proportional to the cost difference between each mode with a constant coefficient μ . The travelers' departure time and mode choices can then be defined as follows:*

$$f_i^{(n+1)} = f_i^{(n)} + \mu \left(c_{b,p}^{(n+1)} - c_{a,p,i}^{(n+1)} \right), \quad \text{for } i = 1, 2, \dots, M \quad (28)$$

and

$$N_b^{(n+1)} = N_b^{(n)} - \mu \sum_{i=1}^M \left(c_{b,p}^{(n+1)} - c_{a,p,i}^{(n+1)} \right). \quad (29)$$

Assumption 4. *The traffic flows only evolve in the interior of the feasible flow set $\bar{\Omega}$, in other words, the traffic flows are always positive.*

Assumptions 3 and 4 are adopted to relax the doubly dynamical model to be differentiable over its feasible set $\bar{\Omega}$. Based on these assumptions, we then can analyze the stability of the stationary point under Eqs.(26)-(29). At the fixed-point (stationary point), $\bar{\mathbf{f}}^{(n)} = \bar{\mathbf{f}}^{(n+1)} = \bar{\mathbf{f}}^*$

and $\mathbf{c}_p^{(n)} = \mathbf{c}_p^{(n+1)} = \mathbf{c}_p^*$, where $\mathbf{c}_p^{(n)} = (c_{a,p,1}^{(n)}, c_{a,p,2}^{(n)}, \dots, c_{a,p,M}^{(n)}, c_{b,p}^{(n)})$. The following Proposition A.1 elaborates the existence and uniqueness of the stationary point.

Proposition A.1. *The dynamical system (26) to (29) has a unique travel flows and perceived travel cost at the fixed point $(\bar{\mathbf{f}}^*, \mathbf{c}_p^*)$.*

Proof. At the fixed point, based on $\bar{\mathbf{f}}^n = \bar{\mathbf{f}}^{n+1}$, $\mathbf{c}_p^{(n)} = \mathbf{c}_p^{(n+1)}$ and Eqs.(26)-(27), we can obtain $\mathbf{c}_p^{(n)} = \mathbf{c}(\bar{\mathbf{f}}^{(n)})$. Also based on Eqs.(28) and (29) we can obtain $c_{b,p}^{(n+1)} = c_{a,p,i}^{(n)}$ for $i = 1, 2, \dots, M$. Then the traffic flows at the stationary point satisfy

$$c_{b,e}(N_b^*) = c_{a,e,i}(f_i^*) \quad \text{for } i = 1, 2, \dots, M. \quad (30)$$

With reference to Lindsey (2004), the solution exists and is unique as

$$f_i = \begin{cases} \frac{\alpha}{\alpha-\beta}sl & t^* - \frac{\gamma}{\beta+\gamma} \frac{N_a^*}{s} \leq il \leq t^* - \frac{\beta}{\alpha} \frac{\gamma}{\beta+\gamma} \frac{N_a^*}{s} \\ \frac{\alpha}{\alpha+\gamma}sl & t^* - \frac{\beta}{\alpha} \frac{\gamma}{\beta+\gamma} \frac{N_a^*}{s} < il \leq t^* + \frac{\beta}{\beta+\gamma} \frac{N_a^*}{s} \end{cases}, \quad (31)$$

and $N_a + N_b = N$. □

Let $\mathbf{J}_c = \mathbf{Jac}(\mathbf{c}(\bar{\mathbf{f}}^*))$ denote the Jacobian matrix of the auto and transit travel cost at the stationary point $\mathbf{c}(\bar{\mathbf{f}}^*)$ with respect to the flows at the stationary point $\bar{\mathbf{f}}^*$. According to Assumption 1, \mathbf{J}_c is a positive lower triangular matrix, then \mathbf{J}_c is positive definite. Denote

$$\mathbf{A} = \begin{pmatrix} -1 & 0 & \cdots & 0 & 1 \\ 0 & -1 & \cdots & 0 & 1 \\ \vdots & \vdots & \ddots & \vdots & \vdots \\ 0 & 0 & \cdots & -1 & 1 \\ 1 & 1 & 1 & 1 & -M \end{pmatrix}_{M+1},$$

since \mathbf{A} is a symmetric and zero-row-sum matrix with non-positive diagonal entries and non-negative off-diagonal entries, so it is negative semidefinite. Then $\mathbf{J}_c \mathbf{A}$ is negative semidefinite, and $\mathbf{I} - \eta_e \omega \mathbf{J}_c \mathbf{A}$ is positive definite and invertible. The Jacobian matrix (32) of the dynamical system (26) to (29) takes the following form:

$$\mathbf{J} = \begin{pmatrix} (1 - \eta_e)(\mathbf{I} - \omega \mu \mathbf{J}_c \mathbf{A})^{-1} & \eta_e(\mathbf{I} - \omega \mu \mathbf{J}_c \mathbf{A})^{-1} \mathbf{J}_c \\ \mu(1 - \eta_e) \mathbf{A}(\mathbf{I} - \omega \mu \mathbf{J}_c \mathbf{A})^{-1} & \mu \eta_e \mathbf{A}(\mathbf{I} - \omega \mu \mathbf{J}_c \mathbf{A})^{-1} \mathbf{J}_c + \mathbf{I} \end{pmatrix}_{2(M+1) \times 2(M+1)} \quad (32)$$

The relationship between the eigenvalues of the matrix \mathbf{J} and $\mathbf{J}_c \mathbf{A}$ satisfies the following Proposition A.2.

Proposition A.2. For each of the $M + 1$ eigenvalues γ_k of matrix $\mathbf{J}_c\mathbf{A}$, two eigenvalues $\lambda'_k = \lambda_k$ and $\lambda''_k = \lambda_{M+1+k}$ of matrix \mathbf{J} are the solutions of the quadratic Eq. (33)

$$\lambda^2 - \frac{2 - \eta_e + (\eta_e - \omega) \mu \gamma_k}{1 - \omega \mu \gamma_k} \lambda + \frac{1 - \eta_e}{1 - \omega \mu \gamma_k} = 0, \quad (33)$$

$$i.e. \quad \lambda_{k/M+1+k} = \left(\frac{2 - \eta_e + (\eta_e - \omega) \mu \gamma_k}{1 - \omega \mu \gamma_k} \pm \sqrt{\chi_k} \right) / 2, \quad (34)$$

where

$$\chi_k = \sqrt{\left(\frac{2 - \eta_e + (\eta_e - \omega) \mu \gamma_k}{1 - \omega \mu \gamma_k} \right)^2 - 4 \frac{1 - \eta_e}{1 - \omega \mu \gamma_k}}. \quad (35)$$

The eigenvalues of \mathbf{J} yield the information about the stability of dynamical system (26) to (29). Conditions for local stability of the dynamical system (26) to (29) require that the maximum modulus $|\lambda_k|$ among all the eigenvalues of the Jacobian matrix \mathbf{J} is less than one.

$$\max_{k=1, \dots, 2(M+1)} |\lambda_k| < 1. \quad (36)$$

The quadratic function Eq.(33) shows that the eigenvalues of \mathbf{J} are related to the eigenvalues of $\mathbf{J}_c\mathbf{A}$, the travellers' learning parameter η_e , the choice updating parameter μ and the sensitivity to the forecast cost ω . The eigenvalues of $\mathbf{J}_c\mathbf{A}$ are determined by the traffic system itself. Since $\mathbf{J}_c\mathbf{A}$ is negative semidefinite, the real part of γ_k is non-positive, i.e., $\gamma_{R,k} \leq 0$. Based on Proposition A.2, we can analyze the influence of the information provision on the stability of the system. When all the eigenvalues of $\mathbf{J}_c\mathbf{A}$ are real, the relationship between the relative sensitivity to the forecast cost ω and the stability of the dynamical system (26) to (29) can be established, which is summarized in Proposition A.3.

Proposition A.3. If all the eigenvalues of $\mathbf{J}_c\mathbf{A}$ are real, when $\omega < \frac{\eta_e}{2}$, the dynamical system (26) to (29) is stable if and only if $|\gamma_k| < \frac{4-2\eta_e}{(\eta_e-2\omega)\mu}, \forall k$, and when $\omega \geq \frac{\eta_e}{2}$, the dynamical system (26) to (29) is always stable.

Based on Proposition A.3, we can readily verify the following results on the impact of the η_f on the stability of the bi-modal dynamical system (26) to (29). If all the eigenvalues of $\mathbf{J}_c\mathbf{A}$ are real, when $\eta_f < \frac{\eta_e}{2\kappa}$ the larger η_f is, the condition for stable equilibrium is more relaxed. When $\eta_f \geq \frac{\eta_e}{2\kappa}$, the dynamical system (26) to (29) is always stable. Thus, compared with the situation that travelers are not affected by the forecast cost, the more the travelers value the forecast costs, the more likely stable the dynamical system is.

Note that the proofs of Proposition A.2 and Proposition A.3 follow Li et al. (2017) and thus are omitted here. However, differently the cost $c_{a,e,i}(\mathbf{f}) = c_{a,e,i}(f_1, f_2, \dots, f_i)$ considered

here is non-separable, while [Li et al. \(2017\)](#) considers static traffic assignment in a single day with separable cost functions.

A.2 Flow evolution under different initial solution

This part displays the evolution of flow patterns in the bi-modal network under two different initial flow solutions. We denote these two initial solutions as Case (1) and Case (2), and compare them with the benchmark solution used in Section 4. Particularly, Case (1) adopts a demand profile where the departures of 50% of the total demand is uniformly distributed in $[0,40]$ (min); and Case (2) adopts a demand profile where the departures of 50% of the total demand is uniformly distributed in $[80,120]$ (min); while in the benchmark case, the departures of 50% of the demand are uniformly distributed over $[0,120]$ (min). The other 50% goes to the public transit.

“place Figure 18 about here”

“place Figure 19 about here”

Specifically, Figure 18 and Figure 19 pick up several days (Days 1, 3, 5, 7, 20, 30, 50, 150, and 500) to show the time-varying queue pattern at the bottleneck and the departure-based experienced travel cost of users in Case (1). Figure 20 and Figure 21 further show those for Case (2). Figure 22 then displays the evolution of modal-split and the error terms for the two cases and compare them with the benchmark case. As can be seen, while the evolution details are different from day to day, the convergence speed reflected by the error term evolution is more or less the same for the three cases.

“place Figure 20 about here”

“place Figure 21 about here”

“place Figure 22 about here”

References

- Arnott, R., De Palma, A., and Lindsey, R. (1990). Economics of a bottleneck. *Journal of Urban Economics*, 27(1):111–130.
- Arnott, R., De Palma, A., and Lindsey, R. (1994). The welfare effects of congestion tolls with heterogeneous commuters. *Journal of Transport Economics and Policy*, pages 139–161.

- Ben-Akiva, M., Cyna, M., and De Palma, A. (1984). Dynamic model of peak period congestion. *Transportation Research Part B: Methodological*, 18(4-5):339–355.
- Ben-Akiva, M., De Palma, A., and Kanaroglou, P. (1986). Dynamic model of peak period traffic congestion with elastic arrival rates. *Transportation Science*, 20(3):164–181.
- Bie, J. and Lo, H. K. (2010). Stability and attraction domains of traffic equilibria in a day-to-day dynamical system formulation. *Transportation Research Part B: Methodological*, 44(1):90–107.
- Cantarella, G. E., Velonà, P., and Watling, D. P. (2015). Day-to-day dynamics and equilibrium stability in a two-mode transport system with responsive bus operator strategies. *Networks and Spatial Economics*, 15(3):485–506.
- Cascetta, E. and Cantarella, G. E. (1991). A day-to-day and within-day dynamic stochastic assignment model. *Transportation Research Part A: General*, 25(5):277–291.
- Daganzo, C. F. (1985). The uniqueness of a time-dependent equilibrium distribution of arrivals at a single bottleneck. *Transportation Science*, 19(1):29–37.
- Di, X., Liu, H. X., Pang, J.-S., and Ban, X. J. (2013). Boundedly rational user equilibria (BRUE): Mathematical formulation and solution sets. *Transportation Research Part B: Methodological*, 57:300–313.
- Dixit, V. V. and Denant-Boemont, L. (2014). Is equilibrium in transport pure nash, mixed or stochastic? *Transportation Research Part C: Emerging Technologies*, 48:301–310.
- Guo, R.-Y. and Huang, H.-J. (2016). A discrete dynamical system of formulating traffic assignment: Revisiting smiths model. *Transportation Research Part C: Emerging Technologies*, 71:122–142.
- Guo, R.-Y., Yang, H., and Huang, H.-J. (2017a). Are we really solving the dynamic traffic equilibrium problem with a departure time choice? *Transportation Science*, (in press).
- Guo, R.-Y., Yang, H., Huang, H.-J., and Li, X. (2017b). Day-to-day departure time choice under bounded rationality in the bottleneck model. *Transportation Research Part B: Methodological*, (in press).
- Guo, R.-Y., Yang, H., Huang, H.-J., and Tan, Z. (2015). Day-to-day flow dynamics and congestion control. *Transportation Science*, 50(3):982–997.

- Guo, X. and Liu, H. X. (2011). Bounded rationality and irreversible network change. *Transportation Research Part B: Methodological*, 45(10):1606–1618.
- Hu, T.-Y. and Mahmassani, H. S. (1997). Day-to-day evolution of network flows under real-time information and reactive signal control. *Transportation Research Part C: Emerging Technologies*, 5(1):51–69.
- Huang, H.-J., Liu, T.-L., and Yang, H. (2008). Modeling the evolutions of day-to-day route choice and year-to-year ATIS adoption with stochastic user equilibrium. *Journal of Advanced Transportation*, 42(2):111–127.
- Huff, J. O., Huff, A. S., and Thomas, H. (1992). Strategic renewal and the interaction of cumulative stress and inertia. *Strategic Management Journal*, 13(S1):55–75.
- Iryo, T. (2008). An analysis of instability in a departure time choice problem. *Journal of Advanced Transportation*, 42(3):333–358.
- Kraus, M. (2003). A new look at the two-mode problem. *Journal of Urban Economics*, 54(3):511–530.
- Laih, C.-H. (1994). Queueing at a bottleneck with single-and multi-step tolls. *Transportation Research Part A: Policy and Practice*, 28(3):197–208.
- Li, X., Liu, W., and Yang, H. (2017). Traffic dynamics in a bi-modal transportation network with information provision and responsive transit services. *Transportation Research Part C: Emerging Technologies*, (under review).
- Li, X. and Yang, H. (2016). Dynamics of modal choice of heterogeneous travelers with responsive transit services. *Transportation Research Part C: Emerging Technologies*, 68:333–349.
- Lindsey, R. (2004). Existence, uniqueness, and trip cost function properties of user equilibrium in the bottleneck model with multiple user classes. *Transportation Science*, 38(3):293–314.
- Liu, W. and Geroliminis, N. (2016). Modeling the morning commute for urban networks with cruising-for-parking: an MFD approach. *Transportation Research Part B: Methodological*, 93:470–494.
- Liu, W. and Geroliminis, N. (2017). Doubly dynamics for multi-modal networks with park-and-ride and adaptive pricing. *Transportation Research Part B: Methodological*, 102:162–179.

- Liu, W., Yang, H., and Yin, Y. (2014). Expirable parking reservations for managing morning commute with parking space constraints. *Transportation Research Part C: Emerging Technologies*, 44:185–201.
- Liu, W., Yin, Y., and Yang, H. (2015). Effectiveness of variable speed limits considering commuters long-term response. *Transportation Research Part B: Methodological*, 81:498–519.
- Sandholm, W. H. (2002). Evolutionary implementation and congestion pricing. *The Review of Economic Studies*, 69(3):667–689.
- Small, K. A. (2015). The bottleneck model: An assessment and interpretation. *Economics of Transportation*, 4(1):110–117.
- Smith, M. and Mounce, R. (2011). A splitting rate model of traffic re-routing and traffic control. *Transportation Research Part B: Methodological*, 45(9):1389–1409.
- Smith, M. and Wisten, M. (1995). A continuous day-to-day traffic assignment model and the existence of a continuous dynamic user equilibrium. *Annals of Operations Research*, 60(1):59–79.
- Smith, M. J. (1984). The existence of a time-dependent equilibrium distribution of arrivals at a single bottleneck. *Transportation Science*, 18(4):385–394.
- Tabuchi, T. (1993). Bottleneck congestion and modal split. *Journal of Urban Economics*, 34(3):414–431.
- Tan, Z., Yang, H., and Guo, R.-Y. (2015). Dynamic congestion pricing with day-to-day flow evolution and user heterogeneity. *Transportation Research Part C: Emerging Technologies*, 61:87–105.
- Trench, W. F. (2013). Introduction to real analysis. *Prentice Hall, Englewood Cliffs, NJ*.
- Vickrey, W. S. (1969). Congestion theory and transport investment. *The American Economic Review*, 59(2):251–260.
- Wang, W. W., Wang, D. Z., Zhang, F., Sun, H., Zhang, W., and Wu, J. (2017). Overcoming the Downs-Thomson Paradox by transit subsidy policies. *Transportation Research Part A: Policy and Practice*, 95:126–147.
- Watling, D. (1999). Stability of the stochastic equilibrium assignment problem: a dynamical systems approach. *Transportation Research Part B: Methodological*, 33(4):281–312.

- Wu, W.-X. (2009). Day-to-day departure time adjustment behaviors in a single bottleneck model. *International Conference on Transportation Engineering*, 345:3375–3380.
- Wu, W.-X. and Huang, H.-J. (2014). Equilibrium and modal split in a competitive highway/transit system under different road-use pricing strategies. *Journal of Transport Economics and Policy*, 48(1):153–169.
- Xiao, L.-L., Huang, H.-J., and Liu, R. (2013). Congestion behavior and tolls in a bottleneck model with stochastic capacity. *Transportation Science*, 49(1):46–65.
- Xiao, L.-L., Liu, T.-L., and Huang, H.-J. (2016). On the morning commute problem with carpooling behavior under parking space constraint. *Transportation Research Part B: Methodological*, 91:383–407.
- Xu, H., Yang, H., Zhou, J., and Yin, Y. (2017). A route choice model with context-dependent value of time. *Transportation Science*, 51(2):536–548.
- Xu, M., Meng, Q., and Huang, Z. (2016). Global convergence of the trial-and-error method for the traffic-restraint congestion-pricing scheme with day-to-day flow dynamics. *Transportation Research Part C: Emerging Technologies*, 69:276–290.
- Yang, F. and Zhang, D. (2009). Day-to-day stationary link flow pattern. *Transportation Research Part B: Methodological*, 43(1):119–126.
- Yang, H., Liu, W., Wang, X., and Zhang, X. (2013). On the morning commute problem with bottleneck congestion and parking space constraints. *Transportation Research Part B: Methodological*, 58:106–118.
- Ye, H., Yang, H., and Tan, Z. (2015). Learning marginal-cost pricing via a trial-and-error procedure with day-to-day flow dynamics. *Transportation Research Part B: Methodological*, 81:794–807.
- Zhang, F., Lindsey, R., and Yang, H. (2016). The Downs–Thomson paradox with imperfect mode substitutes and alternative transit administration regimes. *Transportation Research Part B: Methodological*, 86:104–127.
- Zhang, F., Yang, H., and Liu, W. (2014). The Downs–Thomson Paradox with responsive transit service. *Transportation Research Part A: Policy and Practice*, 70:244–263.
- Zhang, J. and Yang, H. (2015). Modeling route choice inertia in network equilibrium with heterogeneous prevailing choice sets. *Transportation Research Part C: Emerging Technologies*, 57:42–54.

Zhang, X., Yang, H., and Huang, H.-J. (2011). Improving travel efficiency by parking permits distribution and trading. *Transportation Research Part B: Methodological*, 45(7):1018–1034.

Zhou, B., Xu, M., Meng, Q., and Huang, Z. (2017). A day-to-day route flow evolution process towards the mixed equilibria. *Transportation Research Part C: Emerging Technologies*, 82:210–228.

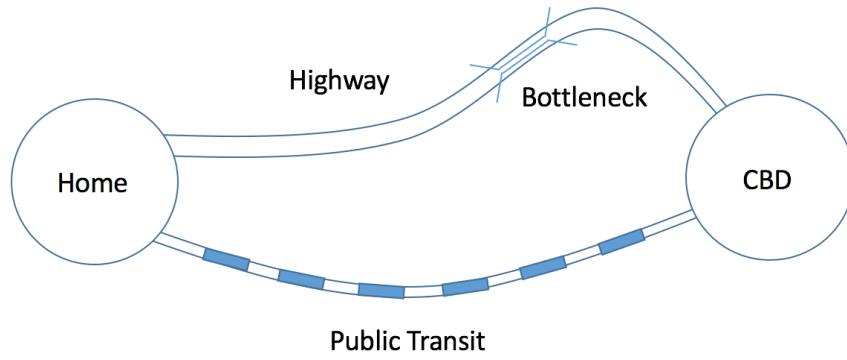


Figure 1: The bi-modal transportation network

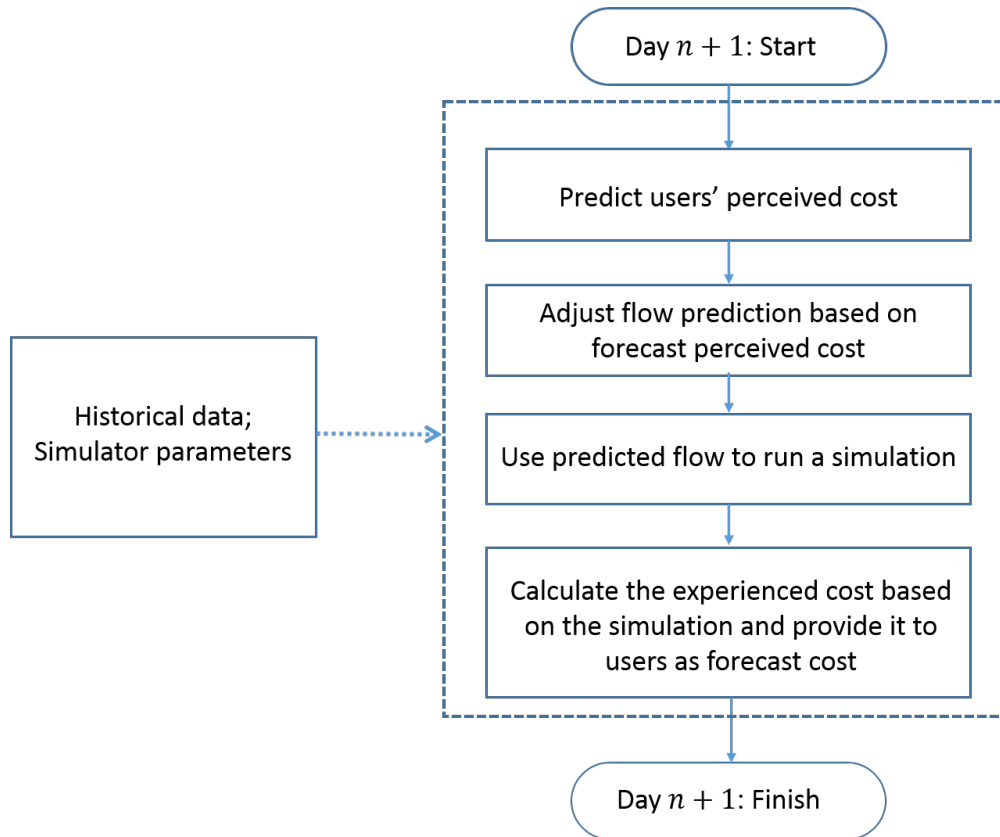


Figure 2: The flowchart for transport agency to determine forecast travel cost

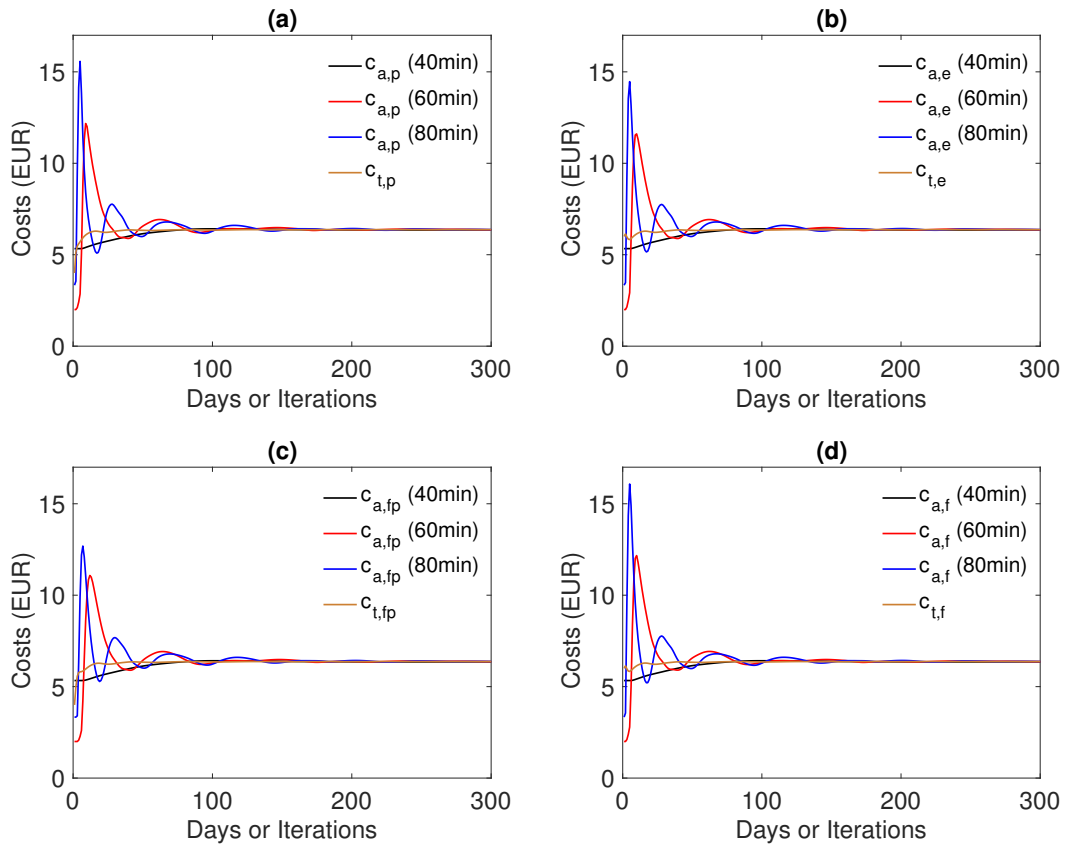


Figure 3: Convergence to User Equilibrium (individual cost evolution)

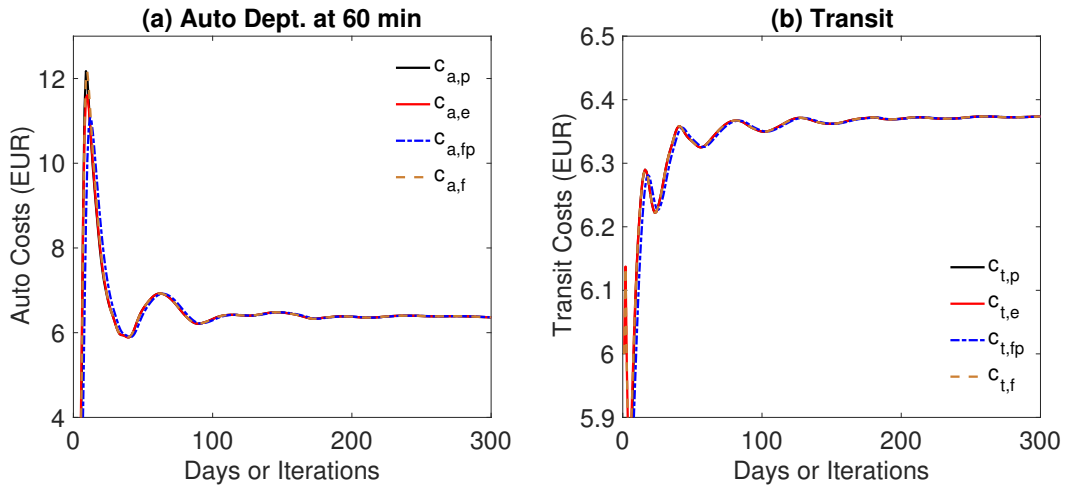


Figure 4: Convergence of different types of costs

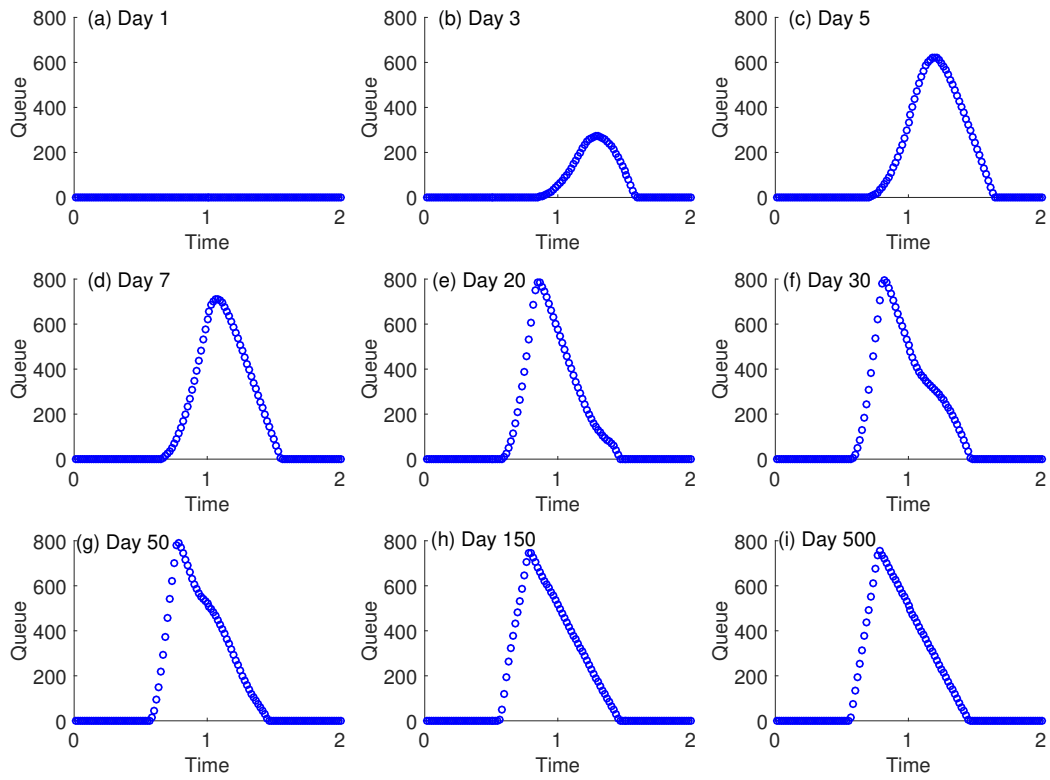


Figure 5: Evolution of time-varying queue length

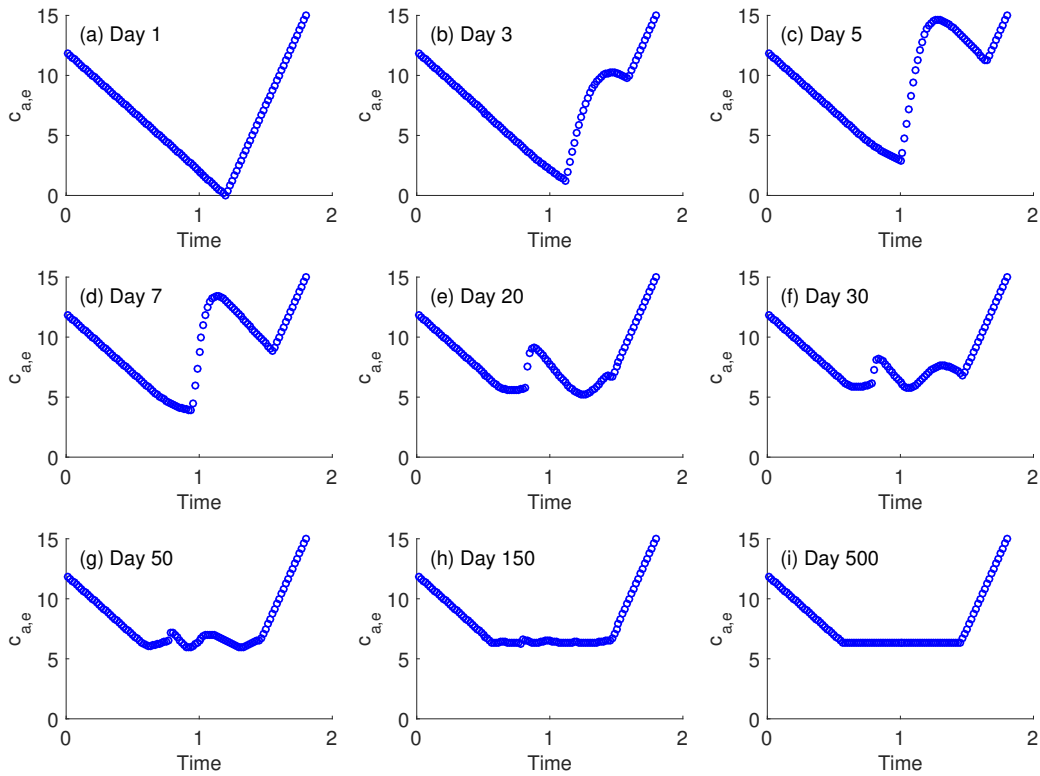


Figure 6: Evolution of (depart-based) time-varying cost

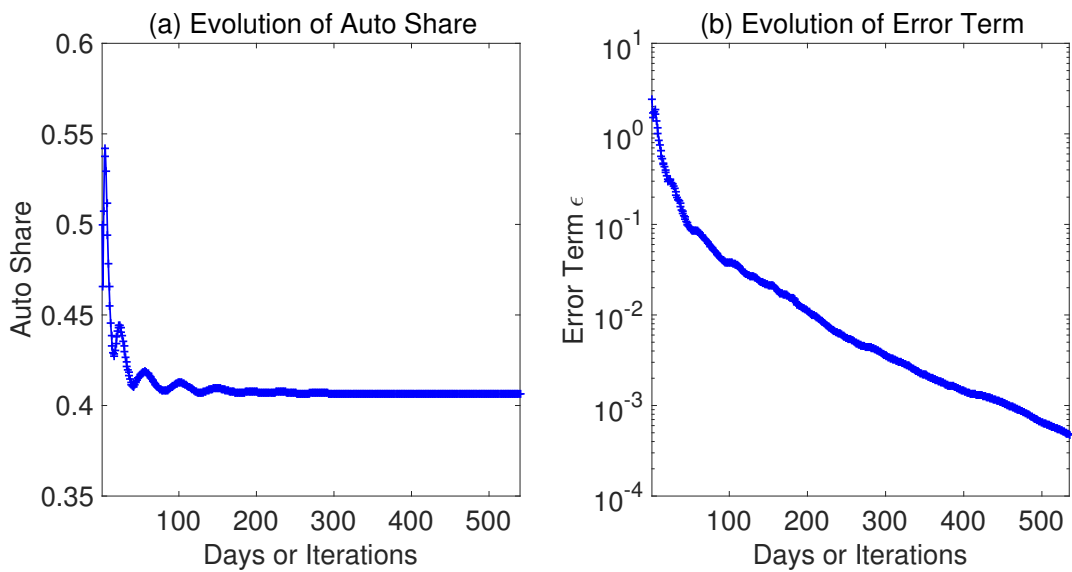


Figure 7: Evolution of auto share and error term ϵ

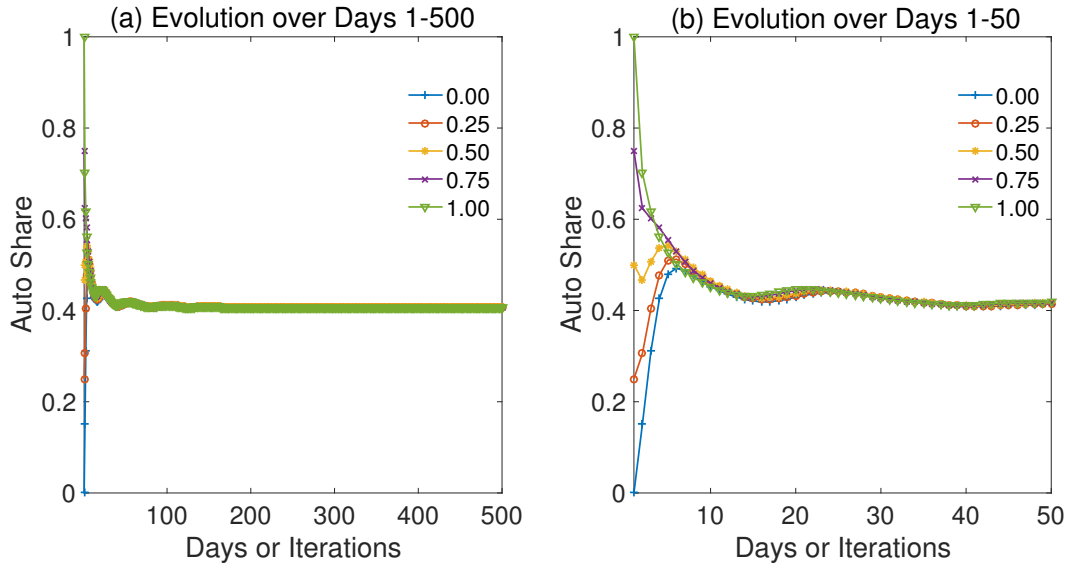


Figure 8: Evolution of modal-split under different initial values

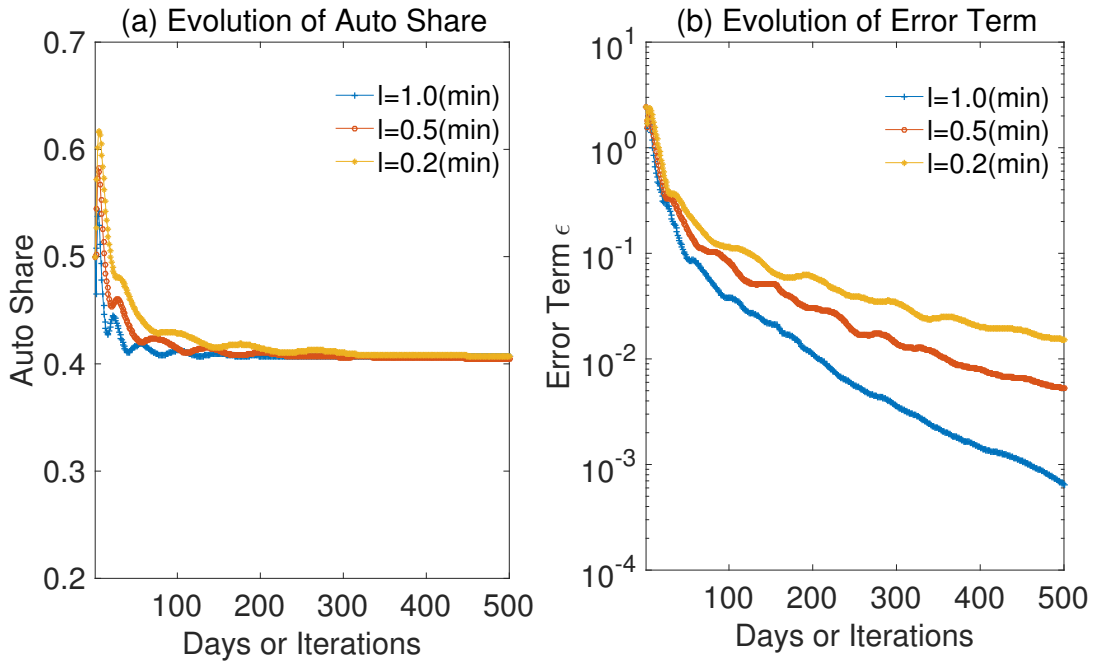


Figure 9: Evolution of modal-splits and error terms under different discretization of clock time

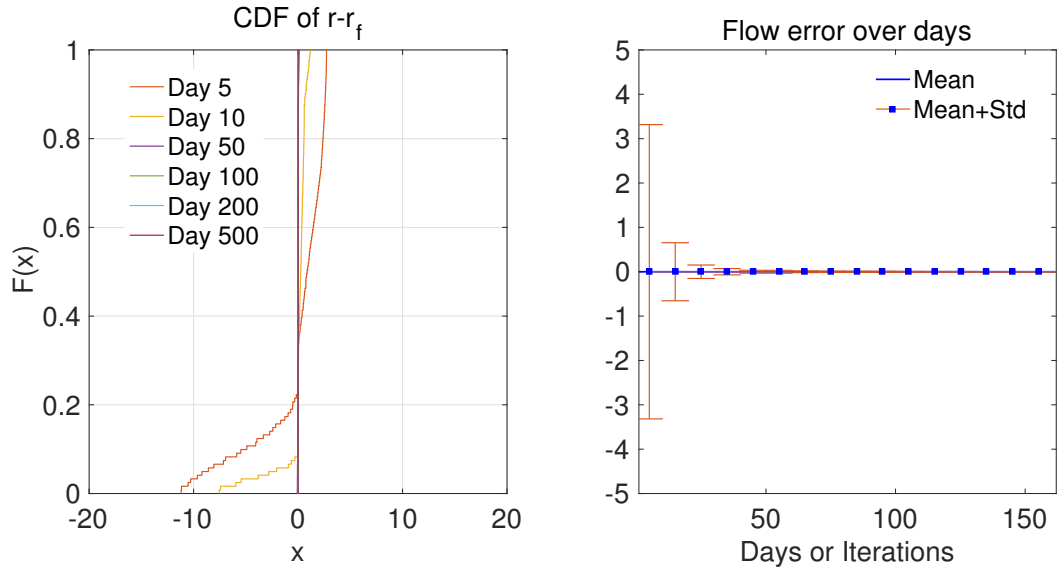


Figure 10: Evolution of forecast flow errors

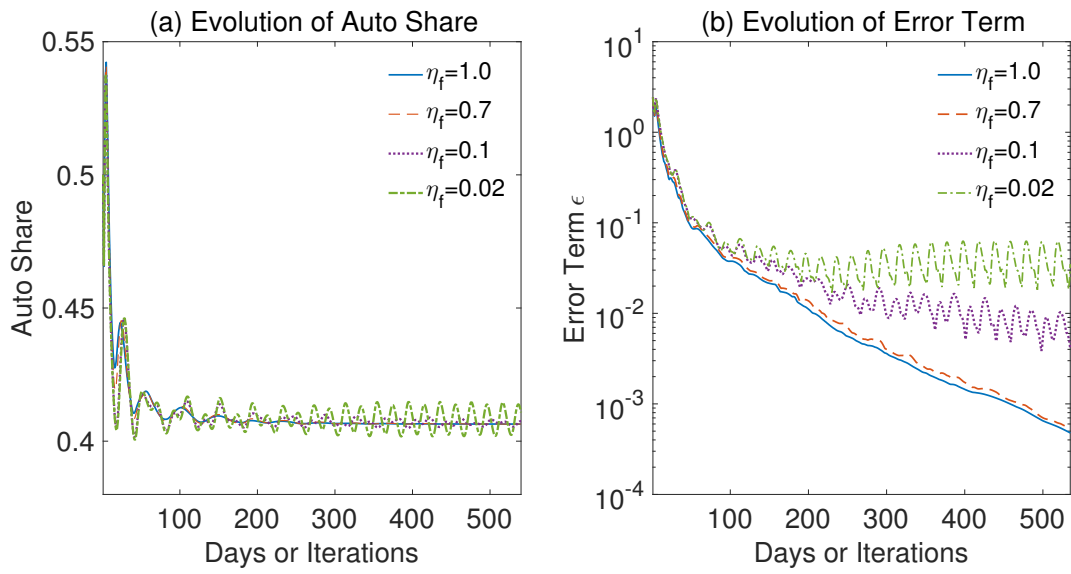


Figure 11: Evolution of modal-splits and error terms under different η_f

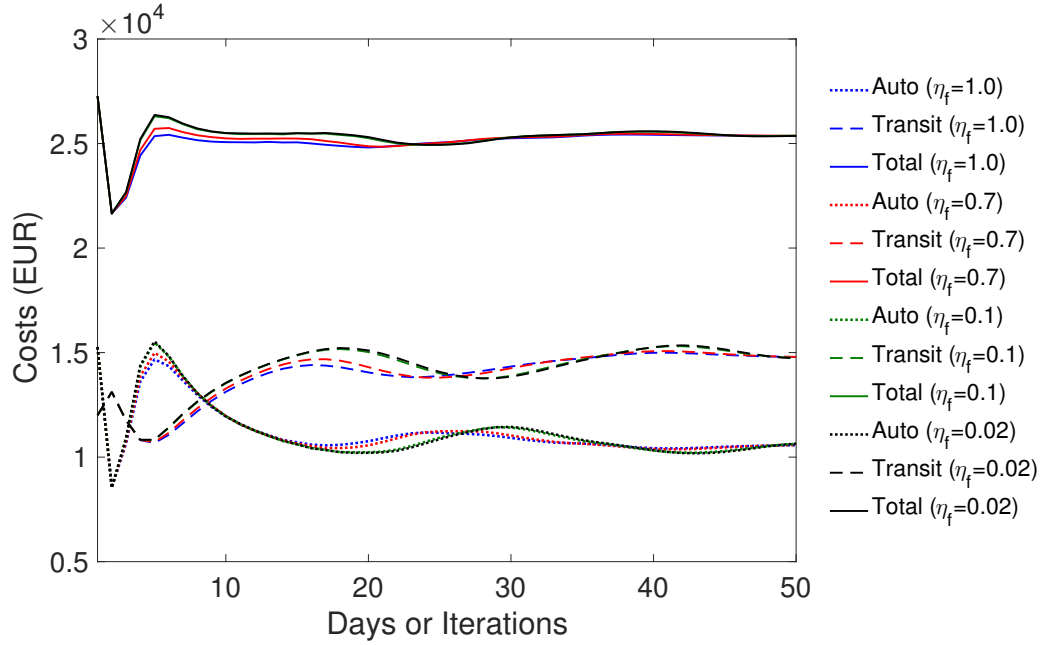


Figure 12: Evolution of system costs under different η_f

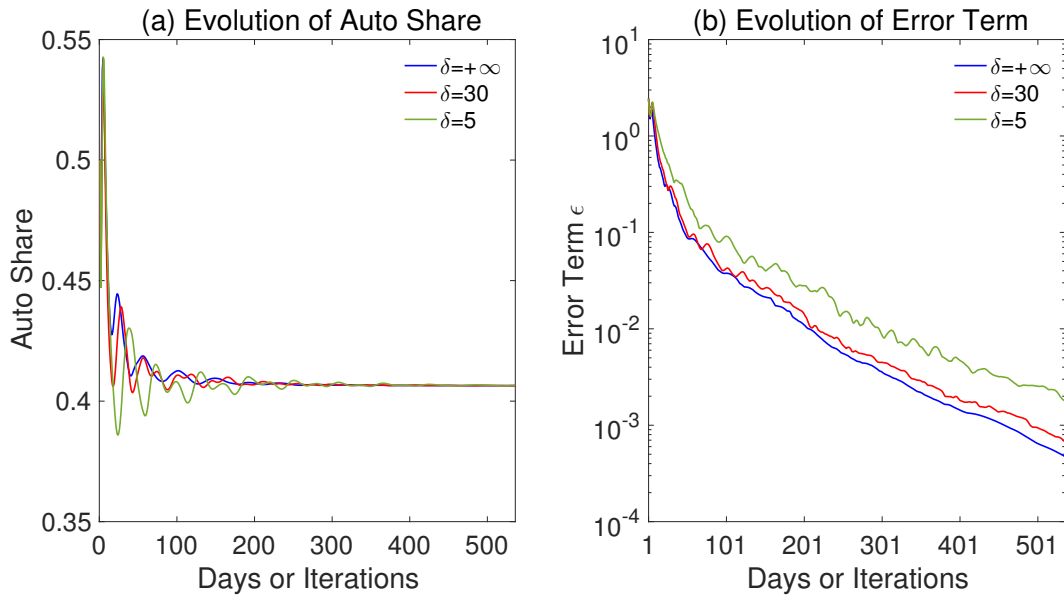


Figure 13: Evolution of modal-splits and error terms under different $\delta (= \frac{\Delta}{t})$

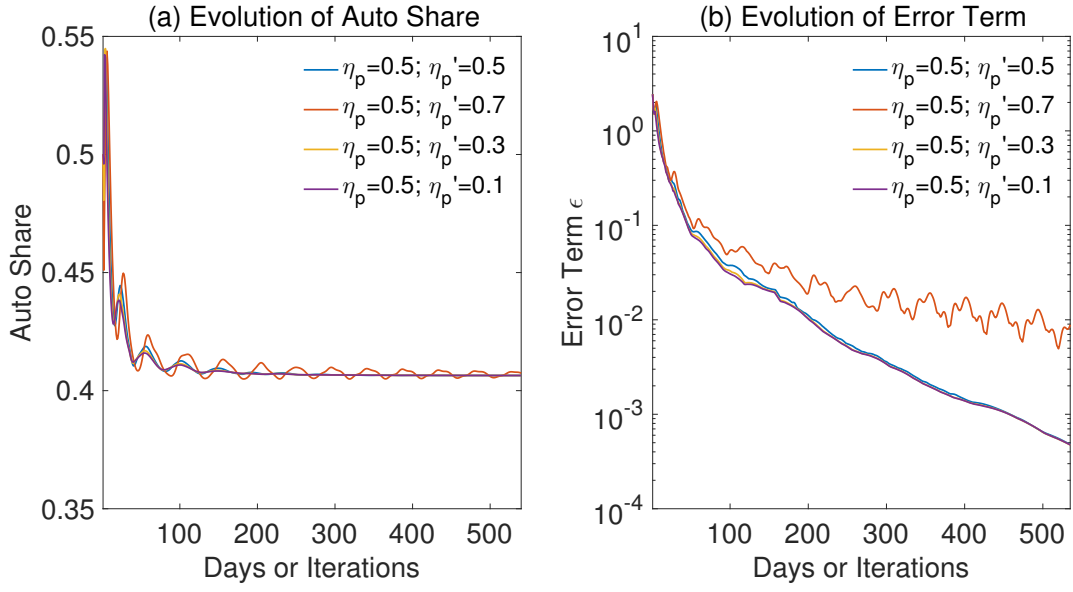


Figure 14: Evolution of modal-splits and error terms under $\eta_p \neq \eta'_p$

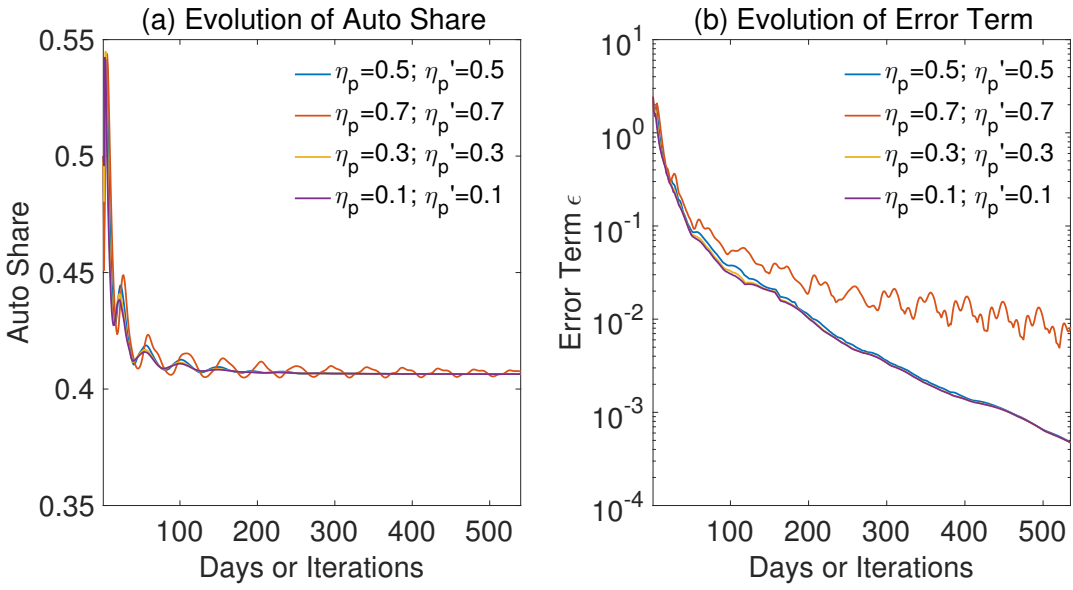


Figure 15: Evolution of modal-splits and error terms under different $\eta_p = \eta'_p$

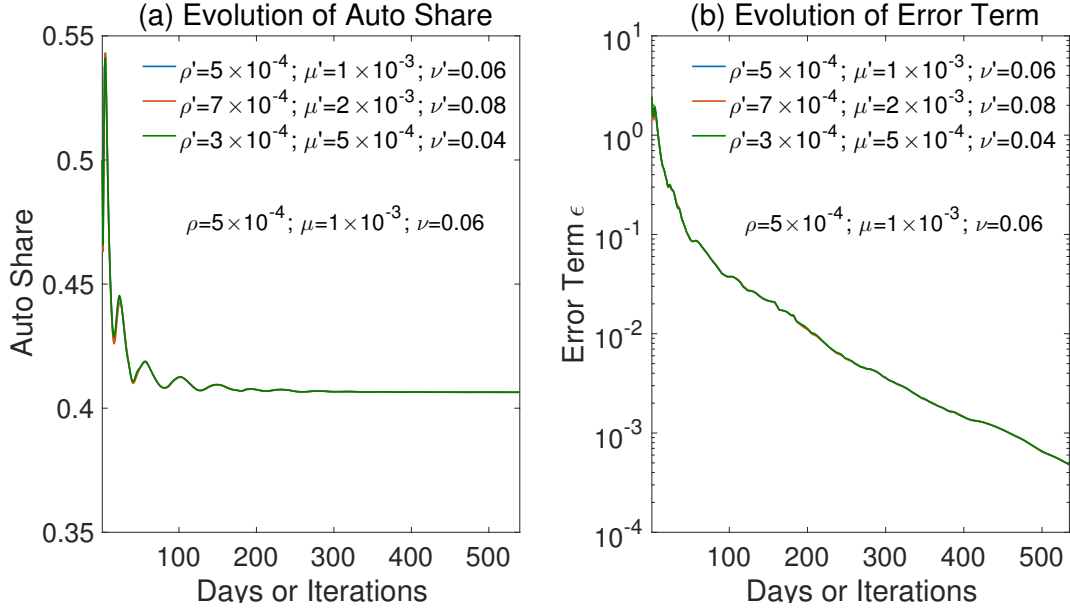


Figure 16: Evolution of modal-splits and error terms under $\rho' \neq \rho$, $\mu' \neq \mu$, and $\nu' \neq \nu$

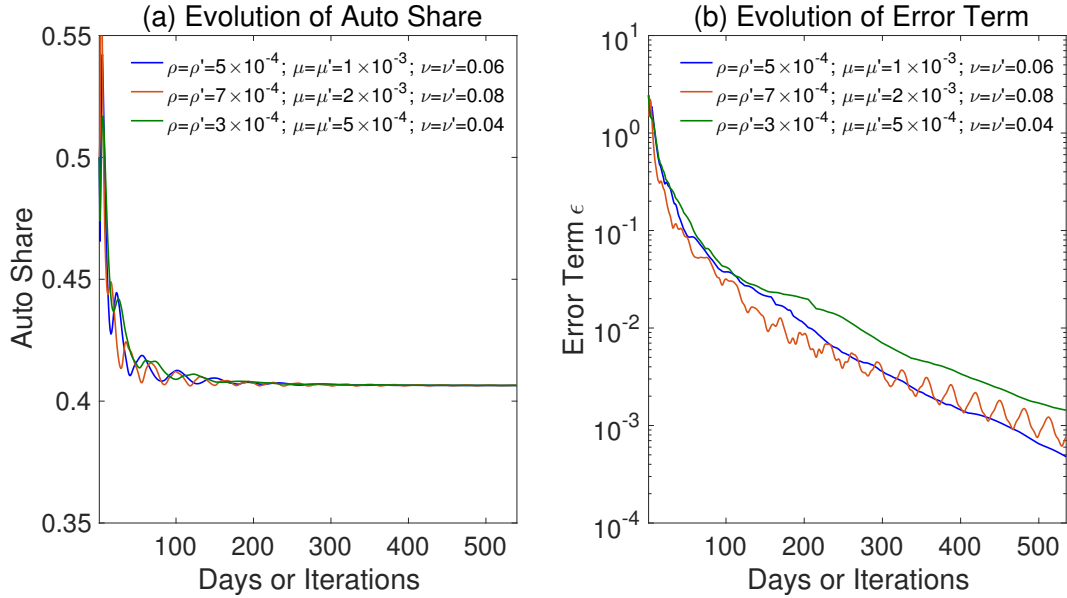


Figure 17: Evolution of modal-splits and error terms under different $\rho' = \rho$, $\mu' = \mu$, and $\nu' = \nu$

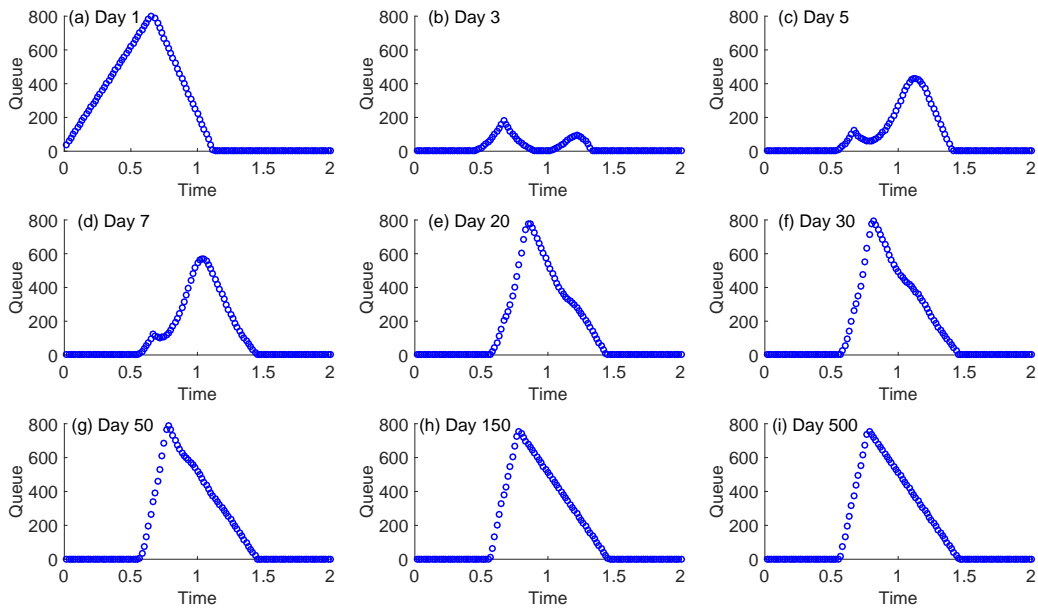


Figure 18: Evolution of time-varying queue length: Case (1)

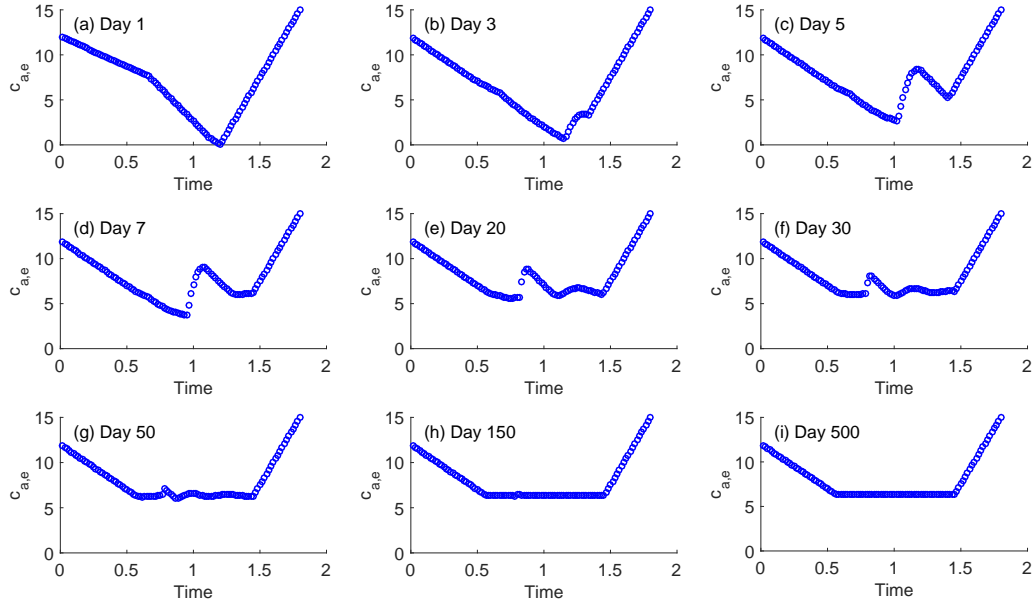


Figure 19: Evolution of (depart-based) time-varying cost: Case (1)

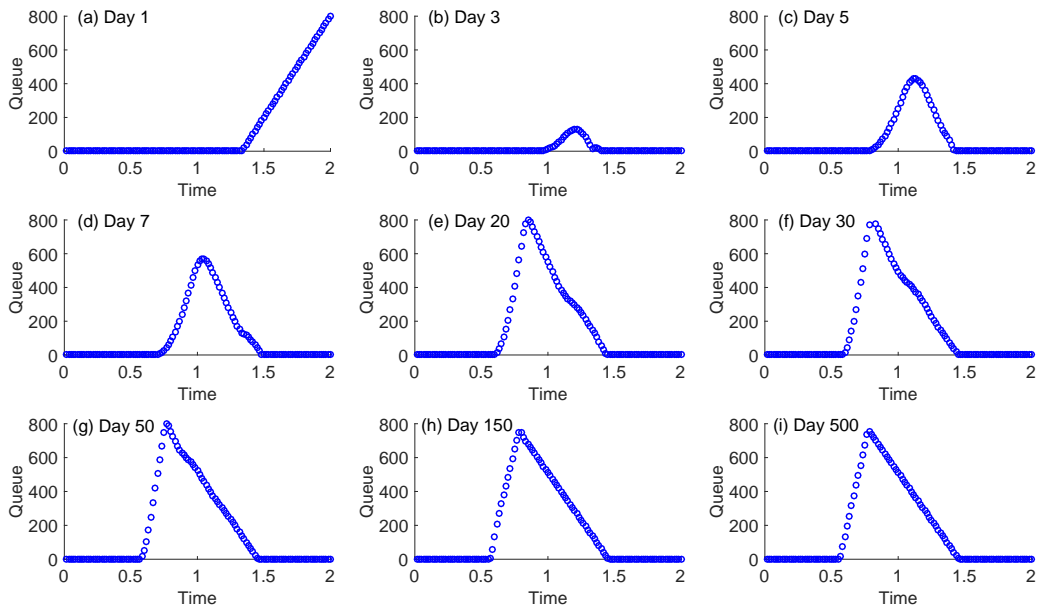


Figure 20: Evolution of time-varying queue length: Case (2)

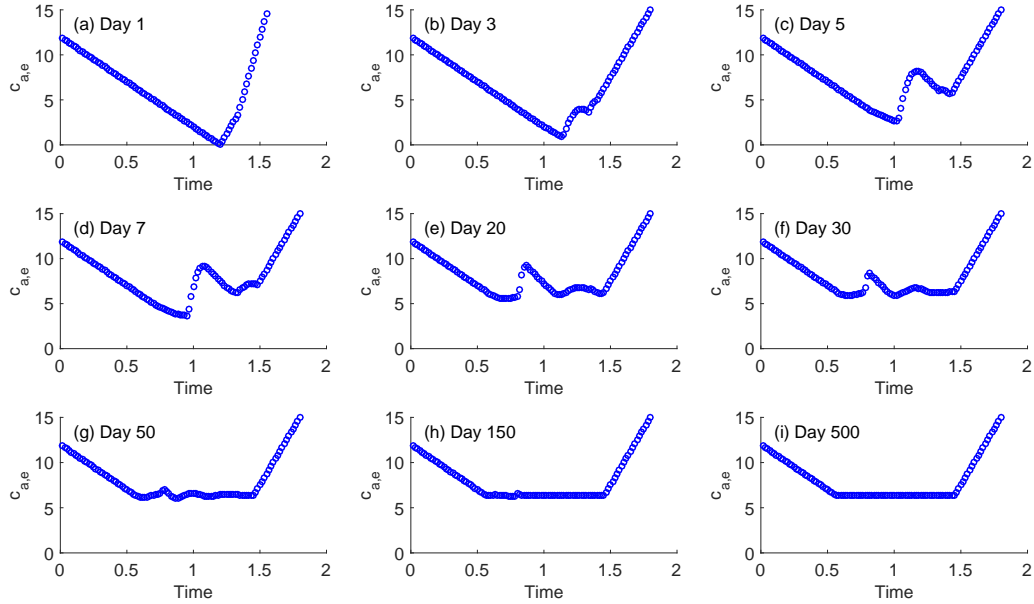


Figure 21: Evolution of (depart-based) time-varying cost: Case (2)

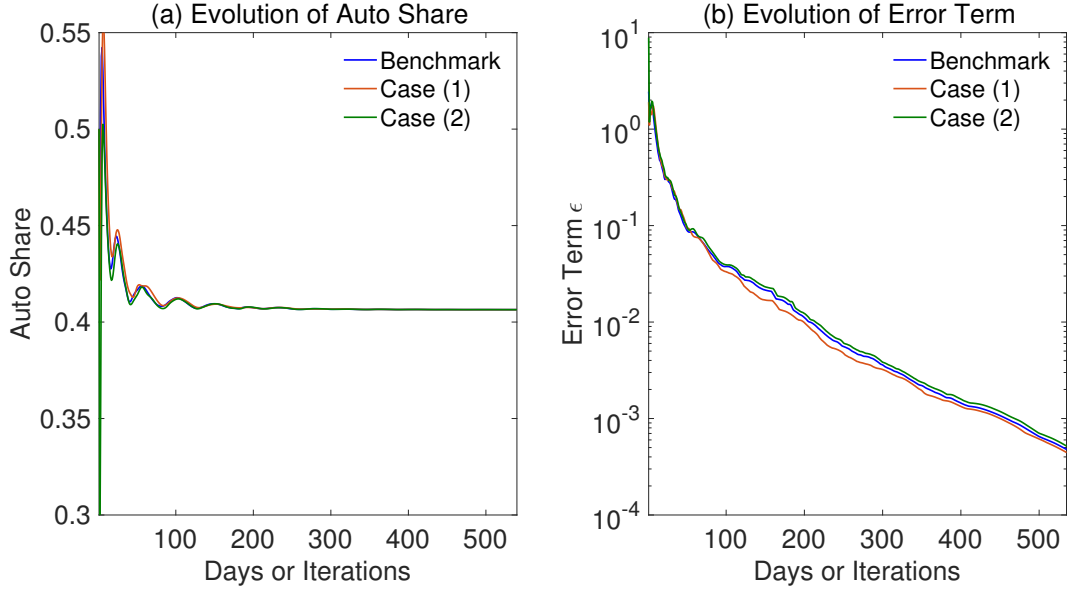


Figure 22: Evolution of modal-split and error terms under the benchmark case and Cases (1) and (2)

Table 1: Summary of basic numerical settings

Parameters or Functions	Specification
Total demand	$N = 4000$
Value of time	$\alpha = 15$ (EUR/hr)
Early arrival penalty	$\beta = 10$ (EUR/hr)
Late arrival penalty	$\gamma = 25$ (EUR/hr)
Highway bottleneck capacity	$s = 1800$ (veh/hr)
Transit cost function	$c_b(N_b) = c_b^0 + c_b^1 \cdot N_b$
Fixed transit cost parameter	$c_b^0 = 4$ (EUR)
Variable transit cost parameter	$c_b^1 = 0.001$ (EUR/user)
Learning parameters	$\eta_p = \eta'_p = 0.5; \eta_e = \eta'_e = 0.5$
Information parameters	$\eta_f = \eta'_f = 1.0;$
Departure time shift coefficients	$\rho = \rho' = 5 \times 10^{-4};$
Mode shift coefficients	$\mu = \mu' = 1 \times 10^{-3}; \nu = \nu' = 0.06;$

List of Figures

1	The bi-modal transportation network	31
2	The flowchart for transport agency to determine forecast travel cost	31
3	Convergence to User Equilibrium (individual cost evolution)	32
4	Convergence of different types of costs	32
5	Evolution of time-varying queue length	33
6	Evolution of (depart-based) time-varying cost	34
7	Evolution of auto share and error term ϵ	34
8	Evolution of modal-split under different initial values	35
9	Evolution of modal-splits and error terms under different discretization of clock time	35
10	Evolution of forecast flow errors	36
11	Evolution of modal-splits and error terms under different η_f	36
12	Evolution of system costs under different η_f	37
13	Evolution of modal-splits and error terms under different $\delta (= \frac{\Delta}{l})$	37
14	Evolution of modal-splits and error terms under $\eta_p \neq \eta'_p$	38
15	Evolution of modal-splits and error terms under different $\eta_p = \eta'_p$	38
16	Evolution of modal-splits and error terms under $\rho' \neq \rho, \mu' \neq \mu, \text{ and } \nu' \neq \nu$	39
17	Evolution of modal-splits and error terms under different $\rho' = \rho, \mu' = \mu, \text{ and } \nu' = \nu$	39
18	Evolution of time-varying queue length: Case (1)	40
19	Evolution of (depart-based) time-varying cost: Case (1)	40
20	Evolution of time-varying queue length: Case (2)	41
21	Evolution of (depart-based) time-varying cost: Case (2)	41
22	Evolution of modal-split and error terms under the benchmark case and Cases (1) and (2)	42

List of Tables

1	Summary of basic numerical settings	42
---	---	----